Review

International Journal of Modern Physics B
Vol. 19, No. 22 (2005) 3415–3473

World Scientific
www.worldscientific.com

DYNAMICS OF BRIGHT MATTER WAVE SOLITONS IN A BOSE–EINSTEIN CONDENSATE

FATKHULLA Kh. ABDULLAEV
Dipartimento di Fisica "E.R. Caianiello", Universitá di Salerno, I-84081 Baronissi (SA), Italy
abdullaev@sa.infn.it

ARNALDO GAMMAL
Instituto de Física, Universidade de São Paulo, 05315-970, C.P. 66318 São Paulo, Brazil
gammal@if.usp.br

ANATOLY M. KAMCHATNOV
Institute of Spectroscopy, Russian Academy of Sciences, Troitsk 142190, Moscow Region, Russia
akamchatnov@yahoo.com

LAURO TOMIO
Instituto de Física Teorica, Universidade Estadual Paulista, Rua Pamplona 145, São Paulo, Brazil
tomio@ift.unesp.br

Received 2 August 2005

Recent experimental and theoretical advances in the creation and description of bright matter wave solitons are reviewed. Several aspects are taken into account, including the physics of soliton train formation as the nonlinear Fresnel diffraction, soliton-soliton interactions, and propagation in the presence of inhomogeneities. The generation of stable bright solitons by means of Feshbach resonance techniques is also discussed.

Keywords: Bose–Einstein condensation; solitons; matter waves.

1. Introduction

Solitons are localized waves that propagate without losing their shape due to equilibrium between dispersion and nonlinearity effects.[1–4] Solitons appear in such physical systems as shallow water, fiber optics and plasma waves. They are typically described by nonlinear equations as the Korteweg–de Vries (KdV) for systems with small dispersion (e.g., shallow water waves), or by the nonlinear Schrödinger (NLS) equation for envelopes of wave packets for the lowest order dispersion and nonlinear effects (e.g., fiber optics and other media). The equation for the "wave

function" of Bose–Einstein condensates (BEC) has the form of multidimensional NLS equation with a trap potential. It is usually known as the Gross–Pitaevskii (GP) equation. In quasi-one-dimensional case, the dynamics of the wave function can be modeled by a one-dimensional (1D) NLS equation, leading to different forms of soliton solutions. Solitons can be classified as bright or dark ones. A bright soliton represents a propagation of wave packets without changing its form. This type of soliton exists for the focusing cubic nonlinearity term corresponding to BEC with attractive interactions between atoms. A dark soliton corresponds to a moving hole on a background that can occur in case of the defocusing cubic nonlinearity, i.e. in BEC with repulsive interactions between atoms.

Bose–Einstein condensates (BEC) were predicted theoretically 80 years ago.[5,6] Only in 1995, after intense experimental research with magnetically trapped weakly interacting atoms, it was reported as evidence that the Bose–Einstein condensation was achieved.[7–9] Since Bose–Einstein condensation is related to the occurrence of macroscopic occupation of a single quantum state, it demonstrates typical quantum mechanical features and, hence, the condensate's motion is often also named as a "matter wave". At zero temperature such condensates of trapped atomic systems can be described in the mean field approximation by the Gross–Pitaevskii (GP) equation[10] (which can be regarded as a non-linear version of the Schrödinger equation for the condensate "wave function" $\Psi(\mathbf{r}, t)$), given by

$$i\hbar\frac{\partial\Psi}{\partial t} = -\frac{\hbar^2}{2m}\nabla^2\Psi + V_{\text{ext}}(\mathbf{r})\Psi + g|\Psi|^2\Psi\,. \tag{1}$$

In the above, m is the single atom mass; the condensate wave function $\Psi \equiv \Psi(\mathbf{r}, t)$ is normalized to the number of atoms N,

$$\int |\Psi|^2 d\mathbf{r} = N\,; \tag{2}$$

$V_{\text{ext}}(\mathbf{r})$ is the external trapping potential that normally can be approximated by a general form of a non-symmetric harmonic oscillator potential,

$$V_{\text{ext}}(\mathbf{r}) = \frac{m}{2}(\omega_x^2 x^2 + \omega_y^2 y^2 + \omega_z^2 z^2)\,; \tag{3}$$

and

$$g \equiv \frac{4\pi\hbar^2 a_s}{m} \tag{4}$$

is the effective coupling parameter associated to the atom-atom interaction, a_s being the s-wave scattering length, and interaction is attractive (repulsive) for $a_s < 0$ ($a_s > 0$). For a condensate in a symmetric trap, with cubic and quintic nonlinear terms, see also Ref. 11.

Since the production of BEC, it was a challenge to demonstrate that solitons could also propagate in such media. The first observation of dark solitons (in BEC with $a_s > 0$) was reported in Ref. 12, followed by experimental observations given in Refs. 13 and 14. Bright matter wave solitons (BS) in BEC can occur when $a_s < 0$.

They are harder to observe than dark solitons due to the occurrence of collapse of the system for sufficiently high number of atoms. Nevertheless, in 2002 two groups, one at Ecole Normale Supériore in Paris[15] and another at Rice University,[16] showed almost simultaneously the generation and propagation of solitons in ^{7}Li condensates. Both experiments are very similar — the main difference is that in the Paris experiment there was much less number of atoms so that only one soliton was formed and its motion in expulsive "anti-trapping" potential was studied, whereas in the Rice experiment trains of several solitons were produced and these trains oscillated in a weak attractive trapping potential. To be definite, we shall describe here in some detail the Rice experiment.[16,17]

We shall first discuss atomic properties of ^{7}Li. As all alkali atoms, the electronic state of ^{7}Li has zero orbital angular momentum and spin momentum $S = 1/2$ so that the total electronic angular momentum is equal to $J = 1/2$. As a result, there is no fine structure of atomic levels due to spin-orbit interaction, but levels have a hyperfine structure originated from the interaction of electronic angular momentum with nuclear spin $I = 3/2$ (or, more exactly, an interaction of electronic and nuclear magnetic moments) of ^{7}Li nucleus. The coupling between the electronic and nuclear spins leads to two possible values $F = I \pm 1/2$ of the total angular momentum $F = 2$ and $F = 1$. Each level in this doublet is $(2F + 1)$-fold degenerate and the hyperfine (hf) splitting between these two levels is given by the Fermi formula[18]

$$\Delta E_{hf} = E_{I+1/2} - E_{I-1/2} = \frac{8\pi}{3} \frac{2I+1}{I} \mu\mu_B \psi_e^2(0)\,, \tag{5}$$

where $\mu_B = e\hbar/2m_e$ is the Bohr magneton, μ is the nucleus magnetic moment, and $\psi_e(0)$ is the normalized valence electron s-wave function at the nucleus. The magnetic moment of ^{7}Li nucleus is positive ($\mu = 3.256\mu_N$, μ_N is the nuclear magneton), hence the ground state corresponds to $F = 1$ and the hyperfine splitting between this level and the higher level $F = 2$ of the doublet is equal to $\nu_{hf} = \Delta E_{hf}/h = 804$ MHz in frequency units or 3.85 K in temperature units. In the presence of a weak magnetic field B these degenerate levels are split into Zeeman multiplets with the energy intervals between sublevels

$$\Delta E = \langle F, m_F | 2\mu_B J_z B | F, m_F \rangle = g_L \mu_B m_F B\,, \tag{6}$$

where we neglect the nucleus magnetic moment due to $\mu_N \ll \mu_B$, and m_F is the eigenvalue of F_z. g_L is the Landé factor given by

$$g_L = \frac{F(F+1) + J(J+1) - I(I+1)}{2F(F+1)}\,. \tag{7}$$

Correspondingly, the mean magnetic moment of the atom is equal to

$$\bar{\mu}_z = -\frac{\partial \Delta E}{\partial B} = -g_L \mu_B m_F\,. \tag{8}$$

For ^{7}Li atom, we have $g_L(F = 2) = 1/4$ and $g_L(F = 1) = -1/4$. Thus, we see that the states $|2, 2\rangle$, $|2, 1\rangle$ and $|1, -1\rangle$ can be trapped by the magnetic trap with the

minimum of the field B, whereas the states $|2,-2\rangle$, $|2,-1\rangle$ and $|1,1\rangle$ are repelled from such a field.

Now, in the experiments the condensation of large enough number of atoms with negative interaction constant $g<0$ (that is with negative scattering length $a_s<0$) is followed by its collapse with loss of majority of the atoms. Therefore one has to condense atoms with positive interaction constant $g>0$ (or $a_s>0$) and after that reverse its sign by changing the atom-atom interaction constant from repulsive to attractive. This can be achieved by means of a Feshbach resonance.[19] A Feshbach resonance occurs when the energy of a pair of colliding atoms matches with the energy of a vibrational state of a diatomic molecule. When one varies an external magnetic field B, the Zeeman energy (5) of atoms changes relative to the energy of a molecule because its magnetic moments differs from that (8) of atoms. Near the resonance the scattering length a_s as a function of the driving magnetic field B can be approximated as

$$a_s = a_b\left(1-\frac{\Delta}{B-B_0}\right), \tag{9}$$

where Δ denotes the width of the resonance. Hence, the external magnetic field allows one to tune the scattering length continuously from $a_s<0$ to $a_s>0$. In ^{7}Li atoms a Feshbach resonance takes place for the state $|F,m_F\rangle=|1,1\rangle$ at $B_0=725$ G and a zero crossing of the scattering length a_s is at $B=550$ G. However, as we saw above, this state is not magnetically trappable, and it is obtained in the final stage of the experiment after several preliminary stages of preparation of the condensate which are described briefly below.

Lithium at room temperature is solid, so it must be heated on up to 900 K to be in the gaseous phase. In the experiment described in Ref. 16 the Lithium sample is diffused through a Zeeman slower and loaded to a magneto-optical trap where the temperature is around 200 μK. These atoms are transferred to a Ioffe–Pritchard magnetic trap in the $|F=2,m_F=2\rangle$ spin state and cooled by evaporation until a temperature of around 1 μK. The atoms are transferred to an optical trap with infrared Nd:YAG laser (1064 nm) focused to a $1/e^2$ intensity radius of 47 μm and power of up to 750 mW for radial confinement. Two cylindrically focused doubled Nd:YAG beams (532 nm) 250 μm apart provide axial confinement. The magnetic trap is then turned off and a uniform magnetic field is ramped to 700 G. The atoms are turned from $|F=2,m_F=2\rangle$ state to $|F=1,\ m_F=1\rangle$ state by an adiabatic microwave sweep of 15 ms and 1 MHz width at $\approx$ 820 MHz. At that magnetic field the scattering length has the large and positive value of $a_s\approx 200a_0$, where a_0 is the Bohr radius that facilitates collisions, since thermalization rate scales as a_s^2. The intensity of the infrared red is then halved. This resulted in trap frequencies $\omega_\perp=\omega_x=\omega_y=2\pi\cdot 640$ Hz, $\omega_z=2\pi\cdot 3.2$ Hz. The gas cools by evaporation with collisions enhanced by a large scattering length, generating a stable BEC. Absorption images indicates that condensates are formed up to $\sim 3\times 10^5$ atoms. Finally, bright solitons are generated by turning the scattering length

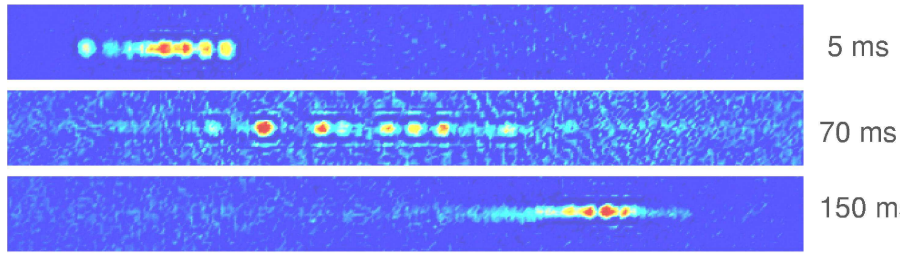

Fig. 1. Repulsive interactions between solitons, as obtained in the experiment described by Strecker *et al.*[16] The images shown a soliton train near the turning points and near the centre of the oscillation.

to near 547 G for which $a \approx -3a_0$, where a_s is small and negative (see Fig. 1). After their generation, the solitons oscillate within an amplitude of ~ 370 μm and period of 310 ms. Image distortion limits the precision of the number of atoms measurement. Solitons have a maximum number of ~ 6000 atoms, in agreement with the maximum allowed by theory.[20–22] Summing up the total number of atoms in the train obtained was less than 6×10^4, indicating that a strong loss occurred in short time compared with the experimental time scale of 30 ms. This losses are caused by collapse and are still to be quantitatively estimated. It was observed that an approximately linear relation exists between the number of solitons produced and the release time from the end caps from $\Delta t = 0$ (four solitons) to $\Delta t = 35$ ms (ten solitons), indicating that the number should vary with the initial size of condensate.

In the following we describe the theory of bright matter waves solitons in elongated cigar-shape trap with attractive atom-atom interactions.

2. One-Dimensional Reduction of Gross–Pitaevskii Equation for Condensates in Cigar-Shaped Trap

When a condensed atomic system is confined in a cigar-shaped trap as given in Eq. (3), with the frequency relations such that $\omega_x = \omega_y \equiv \omega_\perp$ and $\lambda \equiv \omega_z/\omega_\perp \ll 1$, then it is natural to expect that there are situations when transverse degrees of freedom become irrelevant and the GP equation can be reduced to an effective 1D equation. We shall consider this possibility in this section with the aim to clarify characteristic values of the parameters involved into this problem.

If the equation under consideration admits formulation in the form of the Hamiltonian least action principle, with the action functional

$$S = \int L dt\,, \qquad L = \int \mathcal{L} d^3\mathbf{r}\,, \tag{10}$$

then the standard method to eliminate irrelevant degrees of freedom will average the Lagrangian density $\mathcal{L}$ over properly determined space regions or time intervals.

The GP equation admits the Hamiltonian principle formulation with the Lagrangian density

$$\mathcal{L} = \frac{i\hbar}{2}\left(\Psi_t^*\Psi - \Psi_t\Psi^*\right) + \frac{\hbar^2}{2m}\left|\nabla\Psi\right|^2 + V_{\rm ext}(\mathbf{r})|\Psi|^2 + \frac{g}{2}\left|\Psi\right|^4, \tag{11}$$

where $\Psi_t \equiv \partial\Psi/\partial t$. Considering this equation with the corresponding Lagrange equation,

$$\frac{d}{dt}\frac{\partial\mathcal{L}}{\partial\Psi_t^*} + \nabla\frac{\partial\mathcal{L}}{\partial(\nabla\Psi^*)} - \frac{\partial\mathcal{L}}{\partial\Psi^*} = 0\,, \tag{12}$$

one obtains Eq. (1).

In order to obtain a condition under which the transverse degrees of freedom become irrelevant, we have to determine the values of the parameters such that the transverse motion is decoupled from the longitudinal one. A simple inspection of Eq. (1) shows that this aim can be achieved when the characteristic energies of the transverse excitations are much greater than the energy from the nonlinear term. This condition can be written as

$$\frac{\hbar^2}{ms_\perp^2} \sim m\omega_\perp^2 s_\perp^2 \gg g|\Psi|^2\,, \tag{13}$$

where $s_\perp$ is the size of the condensate in the transverse direction. From this, we obtain

$$s_\perp \sim l_\perp, \qquad l_\perp \equiv \sqrt{\frac{\hbar}{m\omega_\perp}}\,. \tag{14}$$

By taking into account Eq. (4) and considering an estimate for the density $|\Psi|^2$ as $|\Psi|^2 \sim N/(s_\perp^2 s_\parallel))$, where $s_\parallel$ is the order of magnitude of the size of the condensate in the longitudinal direction, we obtain the condition

$$\frac{N|a_s|}{s_\parallel} \ll 1\,. \tag{15}$$

It is clear that the estimate (14) means that atoms occupy the ground state of the harmonic motion with the amplitude $l_\perp$ in the transverse oscillator potential, that is, the energies of the longitudinal motion as well as the nonlinear contribution are not high enough to excite the higher levels of the transverse motion in thermodynamic equilibrium. In our case, the transverse motion of atoms is quantized and it reduces to the lowest energy level of the harmonic motion in the transverse potential. Since the transverse motion is reduced to the ground state only so that there is no change of transverse wave function along the cigar axis, we can factorize the whole condensate wave function:

$$\Psi = \phi(x,y)\psi(z,t)\,, \tag{16}$$

where

$$\phi(x,y) = \frac{1}{\sqrt{\pi}\,l_\perp}\exp\left(-\frac{x^2+y^2}{2l_\perp^2}\right) \tag{17}$$

is the ground state wave function of the transverse motion. (We emphasize that this is not a "variational ansatz" with the Gaussian function introduced for convenience in the calculations; here ϕ is the exact ground state wave function, with other states of transverse motion neglected due to Eq. (15).) Thus, we can substitute Eqs. (17) and (16) into Eqs. (11) and (10) and integrate over the transverse xy plane to obtain the expression for the action in terms of an effective only 1D Lagrangian:

$$S = \int L dt\,, \qquad L = \int \mathcal{L}_{1D} dz\,, \tag{18}$$

where, omitting an irrelevant constant term, we have

$$\mathcal{L}_{1D} = \frac{i\hbar}{2}\left(\psi_t^*\psi - \psi_t\psi^*\right) + \frac{\hbar^2}{2m}|\psi_z|^2 + \frac{1}{2}\,m\omega_z^2 z^2|\psi|^2 + \frac{g}{4\pi l_\perp^2}|\psi|^4\,. \tag{19}$$

The Hamiltonian principle states that the evolution of $\psi(z,t)$ is governed by the Lagrange equation (12), which yields the 1D NLS equation

$$i\hbar\,\frac{\partial\psi}{\partial t} = -\frac{\hbar^2}{2m}\,\frac{\partial^2\psi}{\partial z^2} + \frac{1}{2}\,m\omega_z^2 z^2\psi + \frac{g}{2\pi l_\perp^2}|\psi|^2\psi\,, \tag{20}$$

with the normalization condition

$$\int |\psi|^2 dz = N\,. \tag{21}$$

Next, we can estimate the axial size $s_\parallel$ of the condensate. We may consider the situation when the condensate is confined by attractive forces between atoms rather than by the axial trap potential. In this case, its length in the longitudinal direction, $s_\parallel$, can be estimated by equating the dispersive and nonlinear terms:

$$\frac{\hbar^2}{ms_\parallel^2} \sim \frac{g}{l_\perp^2}|\psi|^2 \sim \frac{\hbar^2|a_s|}{ml_\perp^2}\,\frac{N}{s_\parallel}\,, \quad \text{or} \quad s_\parallel \sim \frac{l_\perp^2}{N|a_s|}\,. \tag{22}$$

Actually, this is the width of the bright soliton formed by the condensate. Indeed, neglecting the axial trap ($\omega_z = 0$), Eq. (20) has the well-known solution

$$\psi(z,t) = \sqrt{\frac{|a_s|}{2}}\,\frac{N}{l_\perp}\exp\left[i\frac{mv}{\hbar}\,z - \frac{i}{\hbar}\left(\frac{mv^2}{2} - \frac{\hbar^2\kappa^2}{2m}\right)t\right]\frac{1}{\cosh[\kappa(z-vt)]}\,, \tag{23}$$

where

$$\kappa = \frac{|a_s|N}{l_\perp^2} \sim \frac{1}{s_\parallel} \tag{24}$$

is the inverse width of the soliton and v its velocity. Hence, Eq. (15) implies physically that the soliton width must be much greater than the radial size of the condensate, $l_\perp/s_\parallel \ll 1$. Another convenient form of this condition, obtained using Eq. (22), is given by $N|a_s|/l_\perp \ll 1$.

We can consider the propagation of bright soliton along the trap if its energy is much greater than the potential energy due to the potential at distances $\sim s_\parallel$. That is

$$\frac{\hbar^2}{ms_\parallel^2} \gg m\omega_z^2 s_\parallel^2\,, \quad \text{or} \quad s_\parallel \ll l_\parallel = \sqrt{\frac{\hbar}{m\omega_z}}\,. \tag{25}$$

In this case, using Eq. (22), we obtain

$$\frac{N|a_s|}{l_\perp} \gg \frac{l_\perp}{l_\parallel} = \sqrt{\frac{\omega_z}{\omega_\perp}} = \sqrt{\lambda}\,. \tag{26}$$

Thus, if the conditions

$$\sqrt{\lambda} \ll \frac{N|a_s|}{l_\perp} \ll 1 \tag{27}$$

are fulfilled, the 1D NLS equation can be applied to describe bright solitons moving along a cigar-shape trap. These conditions are to be considered as rough estimates for the applicability of the 1D reduction from three-dimensional (3D) systems in elongated traps. It has been shown numerically in Ref. 20 that a 1D reduction, as well as the ansatz given by Eqs. (17) and (19), is still valid for the cases with $N|a_s|/l_\perp \sim 0.19$ with λ ranging from zero up to 0.4. It is also valid for cases with strong nonlinearity as $N|a_s|/l_\perp \sim 0.38$ with $\lambda = 0$, as justified by multi-scale expansions in Ref. 20.

Note that for condensates that are confined in cigar-shaped traps, with the number N of atoms such that $N|a_s|/l_\perp \geqslant 0.676$, the system collapses[20,22] and the validity of the 1D reduction completely breaks down in agreement with Eq. (27). An improved variational approach, correct beyond the 1D approximation, was suggested in Ref. 23. Its application to bright solitons will be considered in Sec. 6.

3. Formation of Bright Soliton Trains at the Sharp Edge of the Condensate

Formation of bright soliton trains in nonlinear wave systems is often explained as a result of modulational instability, where selection of the most unstable mode is a result of interplay of interference and nonlinear effects (this approach was applied to BEC in e.g. Refs. 24 and 25). Most clearly this process can be seen in the vicinity of a sharp edge of density distribution of BEC. In this case, at linear stage of evolution the linear diffraction provides an initial modulation of the wave and further combined action of interference and nonlinear effects leads to the formation of soliton trains. Without nonlinear effects, such kind of time evolution of a sharp wave front would be a temporal counterpart of usual spatial Fresnel diffraction and therefore soliton train formation at the sharp front of nonlinear wave can be called a nonlinear Fresnel diffraction.

Similar formation of oscillatory structures at sharp wave front or after wave breaking in modulationally stable systems described by the Korteweg-de Vries equation is well known as a "dissipationless shock wave" (see e.g. Ref. 26). Its theoretical

description is given in Refs. 27 and 28, in the framework of Whitham theory of nonlinear wave modulations,[29] where the oscillatory structure is presented as a modulated nonlinear periodic wave which parameters change little in one wavelength and one period. Then slow evolution of the parameters of the wave is governed by the Whitham equations obtained by averaging of initial nonlinear wave equations over fast oscillations of the wave. Description of shock waves generated in BEC with repulsive interaction between atoms was given in Ref. 30. Its application to BEC with attractive interaction was given in Ref. 31 and this theory will be explained here.

As in Sec. 2 we suppose that condensate is confined in a very elongated cigar-shaped trap whose axial frequency ω_z is much less than the radial frequency $\omega_\perp$. In the first approximation, we can neglect the axial trap potential and suppose that condensate is contained in a cylindrical trap ($\omega_z = 0$) and its initial density distribution has a rectangular form. Evolution of BEC is governed by 3D GP equation (1) which under condition (27) can be reduced to 1D NLS equation (20)

$$i\hbar \frac{\partial \psi}{\partial t} = -\frac{\hbar^2}{2m} \frac{\partial^2 \psi}{\partial z^2} + \frac{g}{2\pi l_\perp^2} |\psi|^2 \psi \,, \qquad \int |\psi|^2 dz = N \,. \tag{28}$$

It is well known (see e.g. Ref. 26) that a homogeneous distribution with linear density $n_0 = |\psi(z = 0, t = 0)|^2 = \text{const}$, described by Eq. (28) with negative g ($a_s < 0$) is unstable with respect to self-modulation with an increment of instability equal in the present notation to

$$\Gamma = \frac{\hbar K}{2ml_\perp} \sqrt{8|a_s|n_0 - (l_\perp K)^2} \,, \tag{29}$$

where K is a wavenumber of small periodic modulation. The most unstable mode has the wavenumber

$$K_{\max} = 2\,\frac{\sqrt{|a_s|n_0}}{l_\perp} \tag{30}$$

and the corresponding increment is equal to

$$\Gamma_{\max} = 2|a_s|n_0\omega_\perp \,. \tag{31}$$

This means that after the time $\sim 1/(|a_s|n_0\omega_\perp)$ the homogeneous condensate splits into separate solitons (diffraction fringes) and each soliton (diffraction fringe) contains about $N_s \sim n_0/K_{\max}$ atoms. Hence, the condition of applicability (27) of 1D Eq. (28) to describe the formation of solitons can be expressed as

$$n_0|a_s| \ll 1 \,, \tag{32}$$

which means that the instability wavelength $\sim 1/K_{\max}$ is much greater than the transverse radius $s_\perp$ of BEC. For a typical value of the scattering length $|a_s| \sim 10^{-9} - 10^{-8}$ m this condition is fulfilled, if $N \sim 10^4$ and the initial length of the condensate is about $L \sim 300$ μm so that $n_0 = N/L \sim 3 \cdot 10^7$ m^{-1}. For greater values of n_0 the condition (32) is not satisfied and the transverse motion has to

be taken into account which may lead to the collapse of BEC inside each separate soliton. Therefore we shall confine ourselves to the BEC described by the 1D NLS equation under supposition that the initial distribution satisfies the condition (32).

To simplify the notation, we transform (28) to dimensionless variables $\tau = 2(|a_s|n_0)^2\omega_\perp t$, $\zeta = 2|a_s|n_0 z/l_\perp$, $\psi = \sqrt{2|a_s|}n_0 u$, so that Eq. (28) takes the form

$$iu_\tau + u_{\zeta\zeta} + 2|u|^2 u = 0\,, \tag{33}$$

and u is normalized to the effective length L of the condensate $\int |u|^2 d\zeta = L/l_\perp$ measured in units of $l_\perp$. We study here the process of formation of solitons at the sharp boundary of initially rectangular distribution. Since this process develops symmetrically at both sides of the rectangular distribution, we can confine ourselves to the study of only one boundary. This limitation remains correct until the nonlinear waves propagating inside the condensate collide at its center. If the initial distribution is long enough, this time is much greater than the time of solitons formation. Thus, we consider the initial distribution in the form

$$u(\zeta, 0) = \begin{cases} \gamma \exp(-2i\alpha\zeta)\,, & \text{for } \zeta < 0 \\ 0\,, & \text{for } \zeta > 0\,, \end{cases} \tag{34}$$

where γ is the height of initial step-like distribution and α characterizes the initial homogeneous phase (i.e., initial velocity of the condensate).

Due to dispersion effects described by the second term in Eq. (33), the sharp front transforms into slightly modulated wave which describes usual Fresnel diffraction of atoms. (As was noted above, in our case the diffraction pattern evolves with time rather than is "projected" on the observation plane.) The linear stage of evolution is followed by the nonlinear one in which a combined action of dispersion and nonlinear terms yields the pattern which can be represented as a modulated nonlinear periodic wave or, in other words, a soliton train. We suppose that this soliton train contains large enough number of solitons so that the parameters of the modulated nonlinear wave change little in one wavelength and one period. Then, in framework of Whitham theory, the density of BEC can be approximated by a modulated periodic solution of Eq. (33) (see Ref. 26)

$$n = |u(\zeta, \tau)|^2 = (\gamma + \delta)^2 - 4\gamma\delta\,\mathrm{sn}^2(\sqrt{(\alpha - \beta)^2 + (\gamma + \delta)^2}\,\theta, m)\,, \tag{35}$$

where $\mathrm{sn}(x, m)$ is the Jacobi elliptic function,

$$\theta = \zeta - V\tau\,, \qquad V = -2(\alpha + \beta)\,, \tag{36}$$

$$m = 4\gamma\delta/[(\alpha - \beta)^2 + (\gamma + \delta)^2]\,, \tag{37}$$

the parameters α and γ are determined by the initial condition (34), and β and δ are slow functions of ζ and τ. Their evolution is governed by the Whitham equation

$$\frac{\partial(\beta + i\delta)}{\partial\tau} + v(\beta, \delta)\frac{\partial(\beta + i\delta)}{\partial\zeta} = 0\,, \tag{38}$$

where Whitham velocity $v(\beta, \delta)$ is given by the expression

$$v(\beta,\delta) = -2(\alpha+\beta) - \frac{4\delta[\gamma-\delta+i(\beta-\alpha)]\mathrm{K}}{(\beta-\alpha)(\mathrm{K}-\mathrm{E})+i[(\delta-\gamma)\mathrm{K}+(\delta+\gamma)\mathrm{E}]}\,, \tag{39}$$

$\mathrm{K} = \mathrm{K}(m)$ and $\mathrm{E} = \mathrm{E}(m)$ being the complete elliptic integrals of the first and second kind, respectively. Since our initial condition (34) does not contain any parameters with dimension of length, the parameters β and δ can only depend on the self-similar variable $\xi = \zeta/\tau$. Then Eq. (38) has the solution

$$\frac{\zeta}{\tau} = \xi = v(\beta,\delta) \tag{40}$$

with $v(\beta, \delta)$ given by (39). Separation of real and imaginary parts yields the formulas

$$\frac{\zeta}{\tau} = -4\beta - \frac{2(\gamma^2-\delta^2)}{\beta-\alpha}\,, \tag{41}$$

$$\frac{(\alpha-\beta)^2+(\gamma-\delta)^2}{(\alpha-\beta)^2+\gamma^2-\delta^2} = \frac{\mathrm{E}(m)}{\mathrm{K}(m)}\,, \tag{42}$$

which together with Eq. (37) determine implicitly dependence of β and δ on $\xi = \zeta/\tau$. It is convenient to express this dependence in parametric form

$$\beta(m) = \alpha - \gamma\sqrt{4A(m)-(1+mA(m))^2}\,, \qquad \delta(m) = \gamma m A(m)\,, \tag{43}$$

where

$$A(m) = \frac{(2-m)\mathrm{E}(m)-2(1-m)\mathrm{K}(m)}{m^2\mathrm{E}(m)}\,. \tag{44}$$

Substitution of these expressions into Eqs. (35) and (36) yields the density n as a function of m. Since the space coordinate ζ defined by Eq. (41) is also a function of m at given moment τ, we arrive at presentation of dependence of n on ζ in parametric form. The limit $m \to 0$ corresponds to a vanishing modulation, and this edge point moves inside the condensate according to the law

$$\zeta_- = (-4\alpha + 4\sqrt{2}\gamma)\tau\,. \tag{45}$$

The other edge with $m \to 1$ moves according to the law

$$\zeta_+ = -4\alpha\tau\,, \tag{46}$$

and corresponds to the bright solitons (or fringes of the nonlinear diffraction pattern) at the moment τ. The whole region $\zeta_- < \zeta < \zeta_+$ describes the oscillatory pattern arising due to nonlinear Fresnel diffraction of the BEC with an initially sharp boundary at $\zeta = 0$.

To check the above analytical approach, we have performed numerical simulation of 1D and 3D GP equations. The 1D density distributions calculated numerically from Eq. (33) and given by the above analytical theory are shown in Fig. 2. We see excellent agreement between the theoretical and numerical predictions of the height of the first soliton generated from initially step-like pulse, but its position given by

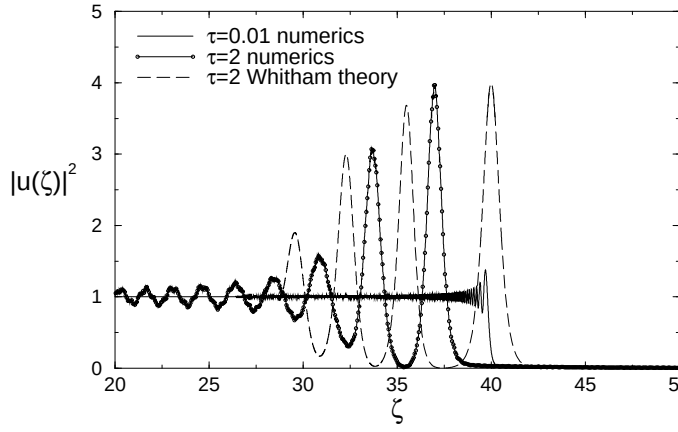

Fig. 2. Density distributions of BEC, calculated by numerical solution of 1D GP equation (33) and given by Whitham theory, with initial step-like wave function (34), with $\gamma = -1$, $\alpha = 0$. Obtained from Ref. 31.

analytical formula is slightly shifted with respect to numerical results. This is a well-known feature of asymptotic Whitham approach[27,28] of which accuracy in the prediction of location of the oscillatory pattern cannot be much better than one wavelength. Thus, we see that the above theory reproduces the numerical results quite well for period of time $\tau \simeq 2$. For much greater time values some other unstable modes different from the one-phase periodic solution (35) can also give considerable contributions into wave patterns. Nevertheless, the qualitative picture of soliton pattern remains the same.

For 3D numerical simulation, the GP equation (1) is written in a dimensionless form in terms of the following non-dimensional variables: $x = l_\perp x'$, $y = l_\perp y'$, $z = l_\perp z'$, $t = 2t'/\omega_\perp$, $\psi = (N^{1/2}/l_\perp^{3/2})\psi$, so that Eq. (1) takes the form

$$i\psi_t = -\Delta\psi + r^2\psi - \frac{8\pi N|a_s|}{l_\perp}|\psi|^2\psi\,, \tag{47}$$

where the primes are omitted for convenience in the notation and the normalization condition is $\int |\psi|^2 2\pi r dr dz = 1$, $r^2 = x^2 + y^2$. Evolution of the density distribution $\rho(z) = \int_0^\infty |\psi(r,z)|^2 2\pi r dr$ along the axial direction is shown in Fig. 3 for the values of the parameters corresponding to the experiment of Ref. 16 ($a_s = -3a_0$, $\omega_\perp = 2\pi \cdot 640$ Hz, $L = 300\, l_\perp$) except for the number of atoms which was chosen to be $N = 5{\cdot}10^3$ in order to satisfy the condition (32) so that $|a_s|n_0 = 1.7{\cdot}10^{-3}$. We see that diffraction (soliton) pattern arises after the dimensionless time $t \simeq 400$ which corresponds after appropriate scaling transformation to $\tau \simeq 2$ in Fig. 2. The width of solitons in Fig. 3 also agrees with the width predicted by 1D analytical theory. The spatial distribution of the condensate density $|\psi(r,z)|^2$ is illustrated in Fig. 4. The 3D nonlinear interference pattern is clearly seen. For greater values of the condensate density, when 1D theory does not apply, numerical simulation demonstrates

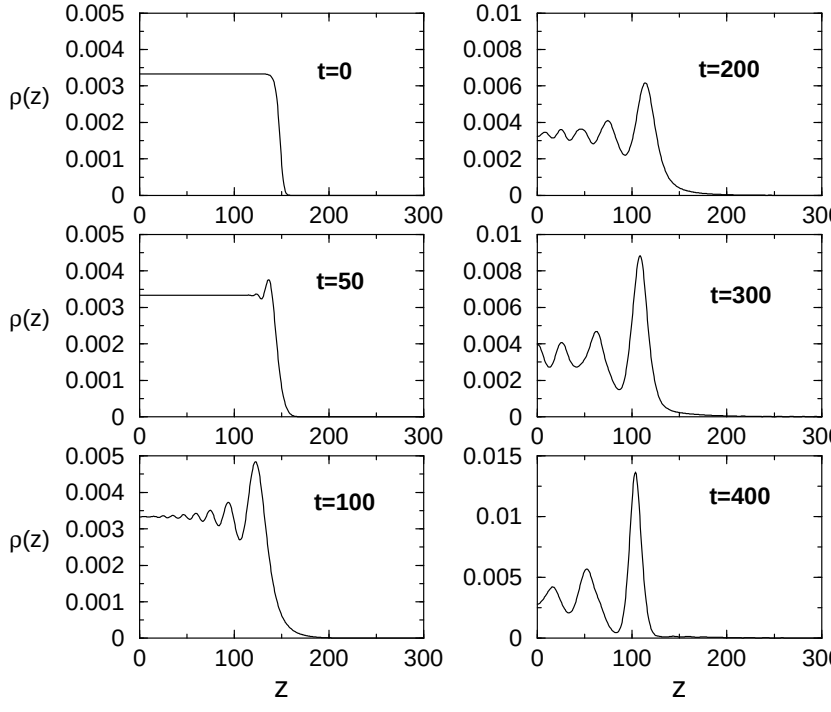

Fig. 3. Density distributions of BEC $\rho(z)$ along axial direction for different moments of time calculated by numerical solution of 3D GP equation (47) with cylindrical initial distribution. Obtained from Ref. 31.

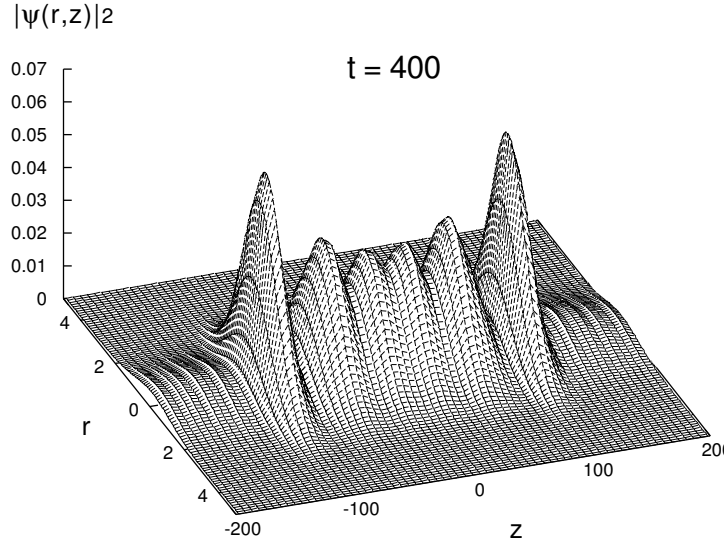

Fig. 4. Dependence of the density distributions on radial, r, and axial, z, coordinates at time $t = 400$. Obtained from Ref. 31.

a similar evolution of the diffraction pattern up to the moment when collapse starts in each separate soliton. Thus, the formation of solitons in the experiment[16] with large initial number of atoms $N \simeq 10^5$ goes through collapses with loss of atoms until the remaining atoms can form stable separate soliton-like condensates. The present theory emphasizes the importance of the initial stage of evolution with formation of the nonlinear Fresnel diffraction pattern.

Formation of soliton trains in BEC confined in a cigar-shaped trap has also been studied numerically in Refs. 24 and 25. The results of 1D simulation of Ref. 25 agree qualitatively with theory presented in Ref. 31. In the numerical results obtained in Ref. 24 strong losses were introduced to prevent fast collapse of BEC with large number of atoms. Nevertheless, formation of soliton trains was also observed.

The above theory is correct for evolution time much less than the period of oscillations $2\pi/\omega_z$ in the axial trap. When the axial trap is taken into account, solitons acquire velocities in the axial direction even if the initial phase is equal to zero. The number of solitons produced ultimately from some finite initial BEC distribution can be found by means of quasiclassical method applied to an auxiliary spectral problem associated with the NLS equation (33) in the framework of the inverse scattering transform method.[28,32] If the initial wave function is represented in the form $u_0(\zeta) = \sqrt{n_0(\zeta)}\,\exp(i\phi_0(\zeta))$, then the total number of solitons is equal approximately to

$$N_s = \frac{1}{\pi}\int \sqrt{n_0(\zeta) + \frac{v_0^2(\zeta)}{4}}\, d\zeta - \frac{1}{2}\,, \tag{48}$$

where $v_0(\zeta) = \partial\phi_0(\zeta)/\partial\zeta$ is the initial velocity distribution of BEC. If there is no imprinted initial phase in BEC, then the total number of solitons is given by

$$N_s = \frac{\sqrt{2|a_s|}}{\pi l_\perp}\int |\Psi| dz\,, \tag{49}$$

which is in dimensional units, neglecting the "one-half" term of Eq. (48).

In the experiments, the initial stage is usually obtained by a sudden change of the sign of the scattering length from positive to negative, so that initial density distribution has, for large enough number of atoms, the Thomas–Fermi form

$$|\Psi|^2 = \frac{3N}{4Z}\left(1 - \frac{z^2}{Z^2}\right), \tag{50}$$

where Z is the Thomas–Fermi half-length of the condensate. Then the substitution of Eq. (50) into Eq. (49) gives

$$N_s = \sqrt{3N|a_s|L}/(4l_\perp)\,, \tag{51}$$

where $L = 2Z$ is the total length of the condensate. Up to a constant factor, this estimate coincides with the one obtained in Ref. 24 by division of L by the instability wavelength $1/K_{\max}$. Note that this estimate includes also very small solitons which cannot be observed in real experiments so that it must be considered as an upper limit of the number solitons which can be produced from a given initial distribution.

The same property of this kind of estimate for the number of dark solitons has been observed in comparison of analytical theory with numerical simulations in Ref. 32. The axial potential mainly influences velocities of solitons so that the above estimate can be applied to the condensate in a cigar-shape trap under the condition that inequality (32) is fulfilled.

4. Adiabatic Formation of Solitons in BEC with Time Dependent Atomic Scattering Length

A powerful tool for generating and managing matter soliton trains can be provided by variation of the effective nonlinearity, as shown in Ref. 33. In practical terms it can be achieved by means of variation of the s-wave scattering length a_s, using Feshbach resonance techniques.[34] The time dependent scattering length $a_s(t)$ is given by replacing B in Eq. (9) by $B(t)$ where $B(t)$ is the time-dependent external magnetic field, Δ is the width of the resonance and B_0 is the resonant value of the magnetic field. Feshbach resonances have been observed in ^{23}Na at 853 and 907 G with $\Delta = 1$ G (Ref. 35), in ^{7}Li at 725 G with $\Delta = 10$ G (Ref. 36), and in ^{85}Rb at 164 G with $\Delta = 11$ G (Ref. 37). We shall show here that in quasi-one-dimensional geometry an initially weak modulation of the condensate can be amplified by means of proper variation of the scattering length. As a result, the condensate with $a_s(t) < 0$ evolves into a sequence of bright solitons.

We start again with 1D Eq. (28) which we transform to the form

$$iu_\tau + u_{\zeta\zeta} + 2g(\tau)|u|^2 u = 0\,, \tag{52}$$

where now $\tau = 2(|a_b|n_0)^2\omega_\perp t$, $\zeta = 2|a_b|n_0 z/l_\perp$, $\psi = \sqrt{2|a_b|}n_0 u$, u is normalized to the number of atoms, and

$$g(\tau) = \frac{a_s(t)}{a_b}\,. \tag{53}$$

We suppose that the initial wave function $u(\zeta, 0)$ is modulated along the cigar axis with the wavelength L of modulation much less than the longitudinal dimension of the condensate. Therefore, at this stage we neglect the smooth trap potential and impose cyclic boundary conditions. Then the initial wave function can be approximated well enough by exact periodic solutions of Eq. (52). We are interested in the evolution of such solutions due to a slow change of $g(\tau)$ with time. At the same time we suppose that the total time of adiabatically slow change of $g(\tau)$ is much less than the period of soliton oscillations in the trap potential so that we can neglect the influence of the trap potential on the motion of solitons during the formation of soliton trains. Correspondingly, the trap potential is omitted in Eq. (52). This means that we shall consider analytically relatively small segments of the modulated wave much greater than the wavelength L and much smaller than the size l of the whole condensate in the trap.

To solve the problem of the condensate evolution, we note that the substitution

$$u(\zeta,\tau)=\frac{v(\zeta,\tau)}{\sqrt{g(\tau)}} \tag{54}$$

transforms Eq. (52) in

$$iv_\tau + v_{\zeta\zeta} + 2|v|^2 v = i\varepsilon v \tag{55}$$

to

$$\varepsilon(\tau)=\frac{1}{2g(\tau)}\,\frac{dg(\tau)}{d\tau}\,. \tag{56}$$

Thus, for slowly varying $g(\tau)$ the right hand side of Eq. (55) can be considered as a small perturbation: $|\varepsilon(\tau)| \ll 1$. As follows from Eq. (54), for the initial distribution one has $v(\zeta,0)=u(\zeta,0)$. For our purposes it is enough to consider typical particular solutions of the unperturbed NLS equation which are parameterized by two parameters $\lambda_{1,2}$. Under the influence of the perturbation, these parameters in the adiabatic approximation become slow functions of time τ. Equations which govern their evolution can be derived by the following simple and direct method.

First, the initial values of λ_i, $i=1,2$, as well as the coefficients in Eq. (55) are supposed to be independent of ζ, hence the wavelength L of the nonlinear wave evolving according to Eq. (55) is constant,

$$\frac{d}{d\tau}L(\lambda_1(\tau),\,\lambda_2(\tau))=0\,. \tag{57}$$

Second, we can easily find that the variable

$$\tilde{N}(\lambda_1(\tau),\lambda_2(\tau))=\int_0^L |v|^2 d\zeta \tag{58}$$

changes with time according to

$$\frac{d}{d\tau}\tilde{N}(\lambda_1(\tau),\lambda_2(\tau))=2\varepsilon\tilde{N}(\lambda_1(\tau),\lambda_2(\tau))\,. \tag{59}$$

Then, if the expressions for L and $\tilde{N}$ in terms of λ_1 and λ_2 are known, Eqs. (57) and (59) reduce to two equations linear with respect to derivatives $d\lambda_1/d\tau$ and $d\lambda_2/d\tau$, which yield the desired system of differential equations for λ_1 and λ_2. The form of this system depends, of course, on the choice of the parameters λ_1 and λ_2. The most convenient choice is provided by the so-called "finite-gap integration method" of obtaining periodic solutions. Therefore we shall use the parametrization of the periodic solutions of the NLS equation obtained by this method (see e.g. Ref. 26), and consider two most typical cases.

Case 1: cn*-wave in a BEC with a negative scattering length*

In the case of a BEC with negative scattering length there are two simple two-parametric periodic solutions of unperturbed Eq. (55). One of them has the form

$$v(\zeta,\tau) = 2\lambda_1 e^{-4i(\lambda_1^2-\lambda_2^2)\tau}\,\mathrm{cn}\left[2\sqrt{\lambda_1^2+\lambda_2^2}\zeta, m\right], \tag{60}$$

where the parameter of elliptic function is given by

$$m = \frac{\lambda_1^2}{\lambda_1^2+\lambda_2^2}. \tag{61}$$

Then straightforward calculations give

$$L = \frac{2\mathrm{K}(m)}{\sqrt{\lambda_1+\lambda_2}}, \qquad \tilde{N} = 8\sqrt{\lambda_1+\lambda_2}\,\mathrm{E}(m) - 4\lambda_2^2 L \tag{62}$$

where $\mathrm{K}(m)$ and $\mathrm{E}(m)$ are complete elliptic integrals of the first and the second kind, respectively. Substitution of these expressions into Eqs. (57) and (59) yields the system

$$\begin{aligned}
\frac{d\lambda_1}{dZ} &= \frac{((\lambda_1^2+\lambda_2^2)\mathrm{E}(m) - \lambda_2^2\mathrm{K}(m))\mathrm{E}(m)\lambda_1}{\lambda_1^2\mathrm{E}^2(m) + \lambda_2^2(\mathrm{K}(m)-\mathrm{E}(m))^2}, \\
\frac{d\lambda_2}{dZ} &= \frac{(\lambda_2^2\mathrm{K}(m) - (\lambda_1^2+\lambda_2^2)\mathrm{E}(m))(\mathrm{K}(m)-\mathrm{E}(m))\lambda_2}{\lambda_1^2\mathrm{E}^2(m) + \lambda_2^2(\mathrm{K}(m)-\mathrm{E}(m))^2}
\end{aligned} \tag{63}$$

where

$$Z = Z(\tau) = 2\int_0^t \varepsilon(\tau')d\tau' = \ln\, g(\tau), \qquad Z(0) = 0. \tag{64}$$

If dependence of λ_1 and λ_2 on Z is found from (63), then Eq. (54) gives evolution of the periodic wave $u(\zeta,\tau)$ with a slow change of the parameter Z connected with time τ by Eq. (64). In particular, the density of particles in the condensate is given by

$$|u|^2 = 4e^{-Z}\lambda_1^2(Z)\,\mathrm{cn}^2\left[2\sqrt{\lambda_1^2(Z)+\lambda_2^2(Z)}\zeta,\, m\right], \tag{65}$$

where transformation to the time variable should be performed with the use of Eq. (64).

In Fig. 5(a) we present an example of the evolution of the respective density distribution. The figure shows that in the case of negative scattering length given by Eq. (9) an increase in the magnetic field $B(\tau)$ within the region $B(0) < B(\tau) < B_0$ results in the compression of the atomic density and the formation of a lattice of matter solitons.

Case 2: dn-*wave in a BEC with a negative scattering length*

Another simple solution of the NLS equation (55) is given by

$$v(\zeta,\tau) = (\lambda_1+\lambda_2)e^{-2i(\lambda_1^2+\lambda_2^2)\tau}\,\mathrm{dn}[(\lambda_1+\lambda_2)\zeta, m]\,, \tag{66}$$

where

$$m = \frac{4\lambda_1\lambda_2}{(\lambda_1+\lambda_2)^2}\,. \tag{67}$$

By analogy with (63) we derive the following equations for λ_1 and λ_2:

$$\begin{aligned} \frac{d\lambda_1}{dZ} &= \frac{\lambda_1(\lambda_1+\lambda_2)\mathrm{E}(m)}{(\lambda_1-\lambda_2)\mathrm{K}(m)+(\lambda_1+\lambda_2)\mathrm{E}(m)}\,,\\ \frac{d\lambda_2}{dZ} &= -\frac{\lambda_2(\lambda_1+\lambda_2)\mathrm{E}(m)}{(\lambda_1-\lambda_2)\mathrm{K}(m)-(\lambda_1+\lambda_2)\mathrm{E}(m)}\,, \end{aligned} \tag{68}$$

where it is supposed that $\lambda_1 > \lambda_2$ and Z is defined by Eq. (64). Now the density of particles is given by

$$|u|^2 = e^{-Z}[\lambda_1(z)+\lambda_2(Z)]^2\,\mathrm{dn}^2[(\lambda_1(Z)+\lambda_2(z))\zeta, m]\,. \tag{69}$$

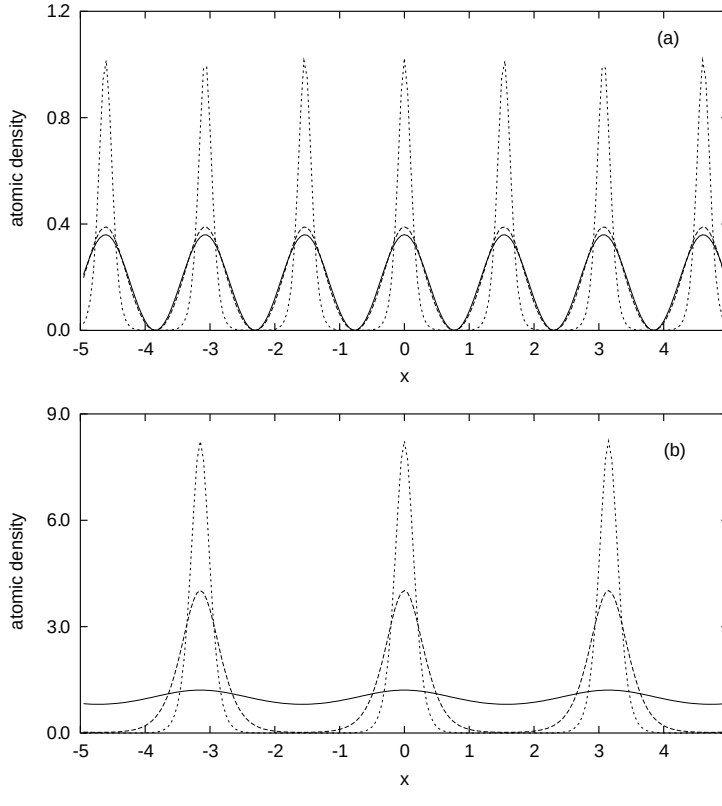

Fig. 5. (a) Evolution of the density distributions: case 1 (cn-wave); (b) case 2 (sn-wave).

An example of the respective evolution is given in Fig. 5(b). Like in the previous case, one observes the formation of a lattice of matter solitons starting with a weakly modulated periodic wave.

Stability of the above solutions has been studied numerically in Ref. 38, where it has been found that soliton trains are stable in the case of positive scattering length and are also stable in the case of negative scattering length for special choice of the parameters. In this context, the adiabatic variation of the scattering length, which results in the change of the wave parameters, can be used for stabilizing (or destabilizing) the respective periodic solution.

5. Propagation and Interactions of Solitons in the Axial Trap

The formation of soliton and the soliton train is followed by its propagation along the axial trap. The investigation of related phenomena required the solution of the GP equation with the different type of traps. While the one-dimensional GP without trap potential and the Schrödinger equation with harmonic potential are integrable models, the joint action of mean field nonlinearity and the trap potential leads in general to a nonintegrable system. Analysis of the soliton dynamics in traps in the form of the double-well or periodic potential shows the appearance of new effects. Indeed, the interaction of solitons interaction in double-well potential induce a chaotic exchange of energy between solitons.[39] The periodic trap — so-called optical lattice — supports gap solitons[40] and discrete breathers.[41,42] Some new phenomena are observed in the interactions of solitons in the harmonic trap. The velocity of propagation and the number of solitons depend on the position of the initial condensate in the harmonic trap (see Sec. 2). After releasing, the solitons are observed to propagate in line as they repel each other. It is well known that bright solitons in the NLS equation show attraction (repulsion) when the relative phase between them is zero (π).[43,44] According to Al Khawaja *et al.*[45] the apparent repulsion of solitons could be explained by "phase imprinting" during formation, where the alternate phase structure of zero and π is provided. The joint action of the harmonic trap and the solitons interaction potential produce the stable configurations in two solitons and N-solitons systems.[46] The control of bright soliton can be performed by the introducing artificial inhomogeneities of linear and nonlinear types, by varying the trap potential in a space and time. The control also can be achieved by the spatial and time variations of the mean field nonlinearity of the GP equation.

It should be noted that at higher densities, the dynamics of nonlinear matter waves start to deviate from one predicted by the one-dimensional NLS equation model. Numerical simulations performed by Salasnich *et al.*[47] showed that due to the presence of the axial trap, the dynamics of solitons is much more complex. In some region of parameters results can be described by 1D GPE with nonpolynomial approximation[48] and more generally by the system of 1D nonlinear equations.[23] We will discuss this case detaily in Sec. 6.

5.1. *Dynamics of bright matter wave solitons with inhomogeneous scattering length*

In order to control the dynamics of bright matter-wave solitons, it was suggested that artificially induced inhomogeneities be used, by considering a variation in the *space* distribution of the atomic two-body scattering length.[49] The condensate with nonlinear impurity is described by the equation

$$\mathrm{i}u_\tau = -u_{\zeta\zeta} + \alpha\zeta^2 u - (1+\varepsilon f(\zeta))|u|^2 u\,, \tag{70}$$

where $\tau \equiv \omega_\perp t/2$ and $\zeta = z/l_\perp$. So, $\varepsilon > 0$ ($\varepsilon < 0$) refers to the negative (positive) variation of the scattering length. Equation (70), for $\alpha = 0$ ($\omega_z \to 0$) and $\varepsilon = 0$, has the soliton solution

$$u^{(s)} = \sqrt{2}A\,\mathrm{sech}[A(z - v\tau)]\mathrm{e}^{\mathrm{i}[\frac{vz}{2} + A^2\tau - \frac{v^2\tau}{4}]}\,, \tag{71}$$

where A is a constant and v is the soliton velocity.

Considering that in the transversal direction we have a much stronger trapping potential ($\omega_\perp \gg \omega_z$), validating an approximation where we average over the x and y directions, we should observe that any different modeling of the impurity in such transversal directions can only bring a multiplicative constant factor in the resulting nonlinear 1D equation. This will result in changing the absolute value of the scattering length or its local space variation (the constant ε). We should also add that the changes in the scattering length will not induce changes in the transverse mode structure; so the averaging procedure over transverse modes is still valid, and the level of applicability is the same as in the case with $\varepsilon = 0$. If we consider modulations of the nonlinear coefficient via, for example, local variation of transverse distribution of trap potential, then the transverse modal structure will change and the 1D approximation can fail.

The 1D Hamiltonian energy corresponding to Eq. (70) is given by

$$\langle H\rangle = \frac{1}{n_0}\int_{-\infty}^{\infty} d\zeta \left[|u_\zeta|^2 + \alpha\zeta^2|u|^2 - \frac{(1+\varepsilon f(\zeta))}{2}|u|^4\right], \tag{72}$$

where n_0 is the normalization of u, related to the number of particles N and the scattering length a_{s0}:

$$n_0 = \frac{4N|a_{s0}|}{l_\perp}\,. \tag{73}$$

To study the dynamics of the perturbed soliton we use the trial function[50]

$$u = A\,\mathrm{sech}\left(\frac{\zeta-\eta}{a}\right)\mathrm{e}^{\mathrm{i}[\phi + w(\zeta-\eta) + b(\zeta-\eta)^2]} \tag{74}$$

where A, a, η, ϕ, w, and b are time-dependent variational parameters. In this case u is normalized to $n_0 = 2aA^2$. To derive the equations for the time-dependent parameters of the soliton, we first obtain the averaged Lagrangian

$$\bar{L}(\tau) = \int \mathcal{L}(\zeta,\tau)d\zeta\,, \tag{75}$$

with

$$\mathcal{L}(\zeta,\tau)=\frac{\mathrm{i}}{2}\left(u_\tau u^*-u_\tau^* u\right)-|u_\zeta|^2-\alpha\zeta^2|u|^2+\frac{1}{2}\left[1+\varepsilon f(\zeta)\right]|u|^4, \tag{76}$$

so that $\bar{L}$ is given by

$$\begin{aligned}\bar{L}=&-n_0\left[\phi_\tau-w\eta_\tau+\frac{\pi^2}{12}\,a^2 b_\tau\right]-\frac{n_0}{3a^2}-n_0 w^2-\frac{\pi^2 n_0 a^2 b^2}{3}\\&+\frac{n_0^2}{6a}+\varepsilon\frac{n_0^2}{8a^2}F(a,\eta)-\alpha n_0\left(\eta^2+\frac{\pi^2}{12}a^2\right),\end{aligned} \tag{77}$$

where

$$F(a,\eta)\equiv\int_{-\infty}^{\infty}d\zeta\frac{f(\zeta)}{\cosh^4(\frac{\zeta-\eta}{a})}\,. \tag{78}$$

and the corresponding Euler-Lagrange equations for the parameters a and η read

$$\begin{aligned}a_{\tau\tau}&=\frac{16}{\pi^2 a^3}-\frac{4n_0}{\pi^2 a^2}-\varepsilon\frac{3n_0}{\pi^2 a^2}\left[2\,\frac{F}{a}-\frac{\partial F}{\partial a}\right]-4\alpha a\,,\\ \eta_{\tau\tau}&=-4\alpha\eta+\varepsilon\,\frac{n_0}{4a^2}\,\frac{\partial F}{\partial\eta}\,.\end{aligned} \tag{79}$$

When a is constant we have the well-known description of motion of the soliton center as the unit mass particle in an anharmonic potential which in the present case is given by $U(\eta)=-\varepsilon(n_0/(4a^2))F(a,\eta)$. For $\varepsilon<0$, to overcome such effective potential barrier, the velocity at $\eta=0$ should be larger than v_c, where $v_c^2=|\varepsilon|n_0/(2a^2)F(a,\eta=0)$. In order to have a more general formulation of the model, we consider a non-zero external potential parameterized by α in the present section. One can also explore the behavior of the soliton by considering a more general time-dependent form of the external potential as studied in Ref. 51. However, here the main motivation is the propagation of matter wave bright solitons in a 1D cigar-like trap,[15,16] so that we assume $\alpha=0$ in the next sections. The applicability of the approach was tested by a comparison between PDE and ODE results. In our case of bright solitons we do not have a problem encountered by the authors of Ref. 52 in the application of the ODE description. In their approach to description of dark solitons they also needed to treat evolution of the background. We note that in Ref. 53 the background influence for the dark soliton in quasi-1D BEC with local *linear* inhomogeneity is considered.

5.2. *Point-like nonlinear impurity*

Let us analyze the system of Eqs. (79), with $\alpha=0$, by first considering a delta-type inhomogeneity ($f(\zeta)=\delta(\zeta)$), and look for the fixed points of such a system. In this case, the approximation for the inhomogeneity can be used when the characteristic scale of the inhomogeneity l_ε is much less than the soliton scale l_s; i.e., when

$$l_s\equiv\sqrt{\frac{l_\perp^2 l_\parallel}{N|a_{s0}|}}=\frac{1}{\sqrt{|a_{s0}|\rho_c}}\gg l_\varepsilon\,, \tag{80}$$

where $\rho_c \equiv N/(l_\parallel l_\perp^2)$ is the condensate density. From Eq. (78), with $f(\zeta) = \delta(\zeta)$, we obtain F and its derivatives:

$$\begin{cases} F(a,\eta) = \operatorname{sech}^4\left(\dfrac{\eta}{a}\right), \\ \dfrac{\partial F}{\partial a} = \dfrac{4\eta}{a^2}\tanh\left(\dfrac{\eta}{a}\right)\operatorname{sech}^4\left(\dfrac{\eta}{a}\right), \\ \dfrac{\partial F}{\partial \eta} = -\dfrac{4}{a}\tanh\left(\dfrac{\eta}{a}\right)\operatorname{sech}^4\left(\dfrac{\eta}{a}\right). \end{cases} \tag{81}$$

The fixed point for the soliton center is given by $\eta = 0$. This corresponds to the case of an atomic matter soliton trapped by the local variation of the two-body scattering length. In case the local variation corresponds to a positive scattering length ($\varepsilon < 0$), we should observe the soliton being reflected by the inhomogeneity. Then, the stationary width a_c can be defined by

$$a_c = \frac{8 - 3\varepsilon n_0}{2n_0}\,. \tag{82}$$

Expanding the solution near a_c we obtain the frequencies of small oscillations for the width a and for the center-of-mass η of the soliton, localized by the impurity. The square of such frequencies are, respectively, given by

$$\begin{aligned} \omega_a^2 &= \frac{4n_0}{\pi^2}\left(\frac{2n_0}{8 - 3n_0\varepsilon}\right)^3 \\ \omega_\eta^2 &= \varepsilon n_0\left(\frac{2n_0}{8 - 3n_0\varepsilon}\right)^4. \end{aligned} \tag{83}$$

In the variational approach, when the soliton collides with the impurity, we have the interaction of the oscillating internal degree of freedom (the width) with the soliton center. As can be seen from Eqs. (83), the frequencies of the oscillations can match, for a certain value of ε, with the energy transfer between the two modes. So, as a result of the reflection from attractive inhomogeneity in BEC, a depinning of the soliton can occur.

5.2.1. *Interface between two BEC media*

Now, we consider another interesting case of an interface between two media such that at $\zeta = 0$ we have a sudden change in the two-body scattering length. The size of the inhomogeneity is given by ε in Eq. (70), where $f(\zeta) = \theta(\zeta)$. In this case, we

have

$$\begin{cases} F(a,\eta) = a\left[\dfrac{2}{3} + \tanh\left(\dfrac{\eta}{a}\right) - \dfrac{1}{3}\tanh^3\left(\dfrac{\eta}{a}\right)\right], \\ \dfrac{\partial F}{\partial a} = \dfrac{F}{a} - \dfrac{\eta}{a}\operatorname{sech}^4\left(\dfrac{\eta}{a}\right), \\ \dfrac{\partial F}{\partial \eta} = \operatorname{sech}^4\left(\dfrac{\eta}{a}\right). \end{cases} \tag{84}$$

And, from Eqs. (79) with $\alpha = 0$, we obtain the coupled equations:

$$\begin{aligned} a_{\tau\tau} &= \frac{16}{\pi^2 a^3} - (\varepsilon+2)\frac{2n_0}{\pi^2 a^2} - \varepsilon\frac{3n_0}{\pi^2 a^2}\left[\tanh\left(\frac{\eta}{a}\right)\right. \\ &\quad \left. - \frac{1}{3}\tanh^3\left(\frac{\eta}{a}\right) + \left(\frac{\eta}{a}\right)\operatorname{sech}^4\left(\frac{\eta}{a}\right)\right], \\ \eta_{\tau\tau} &= \varepsilon\frac{n_0}{4a^2}\operatorname{sech}^4\left(\frac{\eta}{a}\right). \end{aligned} \tag{85}$$

There is no fixed point. At the interface, the value of the width is reduced,

$$a_{\text{int}} = \frac{8}{n_0(\varepsilon+2)}, \tag{86}$$

and the frequency of oscillation of the pulse width is

$$\omega_a = \frac{n_0^2(\varepsilon+2)^2}{16\pi}, \tag{87}$$

or a constant value of a, from the system (85), we obtain

$$\eta_\tau^2 = 2\varepsilon\,\frac{n_0}{4a^2}F(a,\eta) \le \varepsilon\,\frac{2n_0}{3a}. \tag{88}$$

When $a = 4/n_0$ the system (85) reduces to the single equation for η describing the motion of the effective particle, for an optical beam crossing the interface of two nonlinear Kerr media considered in Refs. 54 and 55. If the velocity exceeds the critical value, the soliton pass through the inhomogeneity. An interesting effect, predicted in Ref. 55, can occur when the soliton cross the interface, namely, the possibility of soliton splitting. The soliton is the solution in the first medium. In the second medium it can be considered as the initial wave packet deviating from the solitonic solution for this media. Applying the approach developed in Ref. 28, such an initial condition will decay on few solitons plus radiation.[55] The number of generated solitons is equal to

$$n_{\text{sol}} = \mathcal{I}\left[\frac{1}{\sqrt{2}\pi}\int_{-\infty}^{\infty}|u_0|d\zeta + \frac{1}{2}\right], \tag{89}$$

where u_0 is the initial solution for the second medium, and $\mathcal{I}[\cdots]$ stands for *integer part of* $[\cdots]$. Thus, if we have a jump in the scattering length given by $\Delta a_s = a_{s2} - a_{s1}$, then the number of generated solitons in the second part of the BEC

is equal to $n_{\rm sol} = \mathcal{I}[\sqrt{a_{s2}/a_{s1}} + 1/2]$, where $(1+\varepsilon) = a_{s2}/a_{s1}$ is the ratio of the atomic scattering lengths. For example, for the ratio $9/4 < a_{s2}/a_{s1} < 25/4$ (or $1.25 < \varepsilon < 5.25$) we obtain two solitons in the right-hand-side medium. To obtain $n_{\rm sol}$, we need ε such that $n_{\rm sol}(n_{\rm sol}-1) < (\varepsilon + 3/4) < n_{\rm sol}(n_{\rm sol}+1)$.

5.2.2. *Slowly varying inhomogeneity*

In this subsection, we consider the system of Eqs. (79) for a slowly varying (on the soliton scale) inhomogeneity, given by $f(\zeta) = \exp(-\zeta^2/l_\varepsilon^2)$, with $l_\varepsilon \gg a$. In this case, we obtain the following approximate expressions for $F(a,\eta)$ and its derivatives:

$$\begin{cases} F(a,\eta) \approx \dfrac{4a}{3}\, \exp\left(-\dfrac{\eta^2}{l_\varepsilon^2}\right), \\ \dfrac{\partial F}{\partial a} \approx \dfrac{4}{3}\, \exp\left(-\dfrac{\eta^2}{l_\varepsilon^2}\right), \\ \dfrac{\partial F}{\partial \eta} \approx -\left(\dfrac{8a\eta}{3l_\varepsilon^2}\right) \exp\left(-\dfrac{\eta^2}{l_\varepsilon^2}\right). \end{cases} \tag{90}$$

There is a fixed point at $\eta = 0$, given by

$$a_c = \frac{4}{n_0(1+\varepsilon)}\,. \tag{91}$$

The soliton is trapped by the inhomogeneity for positive ε. In the trapped regime, due to the nonzero chirp, oscillations of the width and oscillations of the center of mass occur. The corresponding frequencies are, respectively, given by:

$$\omega_a = \frac{n_0^2(1+\varepsilon)^2}{4\pi}\,, \tag{92}$$

and

$$\omega_\eta = \sqrt{\frac{\varepsilon(1+\varepsilon)}{6}}\, \frac{n_0}{l_\varepsilon} \overset{l_\varepsilon \gg a}{\longrightarrow} 0\,. \tag{93}$$

Considering an experiment, as in Refs. 15 and 16, with the scattering length of the order of $-3a_0$, and with a variation of about one a_0, we obtain $\varepsilon \sim 1/3$. Taking the critical number $k_\perp = n_0/4 = 0.676$, we obtain $\omega_a \approx 1$, which implies that the characteristic frequency of oscillations of the soliton width is close to $\omega_\perp$ (as the frequencies are given in this unit). And the frequency of oscillation of the center of mass goes to zero with $l_\varepsilon \gg a$, as $\omega_\eta \sim (0.6/l_\varepsilon)$. We note that, the length unit $l_\perp$, for ^{7}Li with $\omega_\perp = 2\pi \times 640$ Hz, is about 1.5 μm. These values for the oscillation frequencies can be experimentally verified.

5.2.3. *Numerical 1D results and variational approach*

Our approach for pulses deviating from the exact soliton solution is interesting from the experimental point of view, considering the difficulty in producing exact

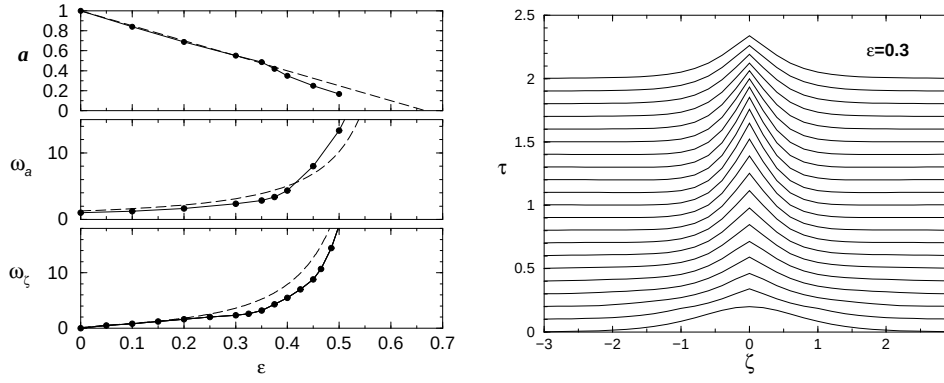

Fig. 6. On the left we show three frames; respectively, from top to bottom, the width a, the frequency of the width oscillations ω_a, and the frequency of the soliton center oscillations ω_η. They are shown as functions of the strength of the nonlinear delta-like impurity ε. Solid line with bullets corresponds to full numerical solution, and dashed line to the corresponding variational approach. On the right, we can see the density profile evolution for a fixed value of the amplitude of the delta-like impurity ε, with arbitrary n_0, in a projected 3D plot. τ and ζ are dimensionless quantities, as given in the text. At $\zeta = 0$, we observe the oscillation of the amplitude, starting from the normal one and going to the nonlinear localized one. Each line represents a fixed τ. For larger ε one can also observe the emission of radiation. All the quantities, in all the frames, are dimensionless and given with appropriate scaling in terms of the normalization n_0. Obtained from Ref. 49.

solitonic solutions. Of particular interest is the non-trivial case of nonlinear Dirac-delta impurity ($f(\zeta) = \delta(\zeta)$), where we made detailed comparison between the variational and full numerical solution of the GP equation. In Fig. 6, in the left, the variation results are compared with the numerical ones, for fixed point of the width, given by a (top frame); for the frequency of oscillations of the width, ω_a (middle frame); and for the frequency of oscillations of the center-of-mass, ω_η, trapped by the inhomogeneity (bottom frame). In this figure, at the right, it is shown numerical simulations of the wave profile.

By using the variational approach, it was observed that the width goes to zero and the frequencies are singular when

$$\varepsilon = \varepsilon_c = \frac{8}{3n_0}\,. \tag{94}$$

Here, it is interesting to observe that we have two critical numbers that are related: one of the critical number $k_\perp = n_{0,\max}/4 \approx 0.676$ comes from the quasi-1D limit of a 3D calculation;[56] another is the maximum amplitude of the delta-like impurity that we have just introduced, given by Eq. (94). Considering both restrictions, the smaller value of ε_c is about one. The plots in the three frames shown in Fig. 6, the left, are obtained for arbitrary values of n_0 (where the maximum is about 8/3, according to Ref. 56), after considering a rescaling in the equations for the width (82) and frequencies (83); and also for ε, such that in the x-axis we consider $(n_0/4)\varepsilon$. From Eq. (94), one obtains $\varepsilon_c(n_0/4) = 2/3$. As shown in this figure, the variational

results are supported by the full numerical calculation. The singularity occurs when the contributions coming from the inhomogeneity and nonlinearity are equal to the contribution from the quantum pressure, as seen from Eq. (79). When $\varepsilon \geq \varepsilon_c$, the collapse of solitary wave occurs. So, we can observe the collapse of a 1D soliton on the attractive nonlinear impurity. This possibility can be obtained following a dimensional analysis in the 1D Hamiltonian given in Eq. (72). The behavior of the field at small widths is $u \sim 1/L^{1/2}$. Taking into account that $\delta(\zeta) \sim 1/L \sim |u|^2$, we can conclude that the contribution of the potential energy due to the impurity is $\sim |u|^6$. For positive ε this term on the impurity exceeds the quantum pressure and leads to the collapse of the soliton. In real situations, the collapse will be arrested on the final stage of the evolution, when the width of the soliton is of the order of the inhomogeneity scale. Then, the delta-function approximation for the impurity will break up.

Observing the numerical simulations of the wave profile, shown in Fig. 6 on the right, we note that, after strong emission of radiation, it evolves into the so-called *nonlinear localized mode*. The nonlinear localized mode represents an *exact* solution of GP equation with nonlinear impurity (70) and it is the nonlinear *standing* atomic matter wave. The solution,

$$u^{(ni)} = \sqrt{2}a\,\mathrm{sech}[a|\zeta| + \beta]e^{\mathrm{i}a^2\tau}\,, \tag{95}$$

where

$$\beta \equiv \beta(\varepsilon, a) \equiv \mathrm{sign}(\varepsilon)\ln(2|\varepsilon|a + \sqrt{1+4\varepsilon^2a^2})^{1/2}\,, \tag{96}$$

can be obtained by using the solution of the homogeneous equation with the requirement of the field continuity at the inhomogeneity and satisfying the jump condition in the first derivative.[57] The normalization $N^{(ni)}$, is

$$\begin{gathered} N^{(ni)} = 4a[1-\varepsilon\gamma]\,, \qquad \gamma \equiv \gamma(\varepsilon, a) \\ \gamma = \frac{\sqrt{1+4\varepsilon^2a^2}-1}{2\varepsilon^2 a} = \frac{2a}{\sqrt{1+4\varepsilon^2a^2}+1}\,. \end{gathered} \tag{97}$$

For small amplitude (or small impurity strength $|\varepsilon|$)

$$N^{(ni)} \approx 4a(1-\varepsilon a)\,. \tag{98}$$

At large amplitudes, we have $N^{(ni)} \to 2/\varepsilon$ for $\varepsilon > 0$; and $N^{(ni)} \to 8a$ for $\varepsilon < 0$. Note that for $\varepsilon < 0$ we have a solution with two-bump structure for the nonlinear localized mode. As shown in Ref. 57, this mode is unstable. Here, we have considered only the case $\varepsilon > 0$. In order to verify the stability of the solutions, one can study the behavior of the second time derivative of the mean-square radius, as in Refs. 57–59. To obtain the second time derivative of the mean-square radius, we use the Virial

approach, with $H = -\partial_{\zeta\zeta} + V$ and $V \equiv -(1 + \varepsilon\delta(\zeta))|u|^2$:

$$\begin{aligned} \langle\zeta^2\rangle_{\tau\tau} &= 4\langle[H, \zeta\partial_\zeta]\rangle = 8\langle(-\partial_{\zeta\zeta})\rangle - 4\langle\zeta V_\zeta\rangle\,, \\ \langle\zeta V_\zeta\rangle &= = -\frac{1}{2}\langle V\rangle + \frac{\varepsilon}{2n_0}|u_0|^4\,, \\ \langle\zeta^2\rangle_{\tau\tau} &= \frac{1}{n_0}\int d\zeta(8|u_\zeta|^2 - 2|u|^4) - \frac{4\varepsilon}{n_0}|u_0|^4\,. \end{aligned} \tag{99}$$

For the system to collapse we need $\langle\zeta^2\rangle_{\tau\tau} < 0$; implying that

$$\varepsilon > \frac{1}{2|u(0)|^4}\int(4|u_\zeta|^2 - |u|^4)d\zeta\,. \tag{100}$$

Using our solitonic ansatz, when $a \to 0$, we reach the critical limit, $\varepsilon_c = 8/(3n_0)$ that was obtained before.

We have also investigated the dynamics of the matter soliton interacting with inhomogeneity, studying different regimes of propagation for several values of ε. In Fig. 7, we present the results of numerical simulations for the final velocity (v_f) versus the initial velocity (v_i) of the soliton, considering different strengths ε for the delta-like inhomogeneity. In this figure and in the next numerical results, considering the general application of the 1D NLS equation with nonlinear impurity, we took $N|a_{s0}|/l_\perp = n_0/4 = 1$, that can easily be rescaled to a value smaller than 0.676, consistent with the BEC quasi-1D results. Considering a factor ξ for the rescaling, as a general rule, we have the following transformations:

$$\begin{aligned} \varepsilon &\to \varepsilon\xi\,, \\ \{\text{length}\} &\to \{\text{length}\}\xi\,, \\ \{\text{time}\} &\to \{\text{time}\}\xi^2\,. \end{aligned} \tag{101}$$

We should note that, the rescaling applied in Fig. 6 was such that $\xi = n_0/4$. In this case, for the velocities, one should make the replacement $v \to v(4/n_0)$ in the plots. As observed in Fig. 7, a region for the velocities where the *attractive* nonlinear impurity reflects the soliton exists. In the model involving the constant width approximation, this region corresponds to the trapped soliton exists. The numerical results show that one window corresponding to the reflection of the soliton always exists. By increasing ε, this window is shifted to larger initial velocities. From the variation of the number N, with respect to the initial velocity v_i (see Fig. 7), one can also observe strong wave emissions by soliton, when ε increases and tends to the critical value (see also Ref. 57). This picture reminds us of the picture of the collapse in 2D BEC with attractive interactions. We note that, by considering the interaction of sine-Gordon kink with attractive defects, many windows were found, corresponding to a resonance with local mode (see Ref. 60). To compare with the results given in the lower frame and left of Fig. 7, we present in Fig. 8, for a fixed value of $\varepsilon = 0.4$, full numerical calculation of the time evolution of the center-of-mass position, considering different values of the initial velocity.

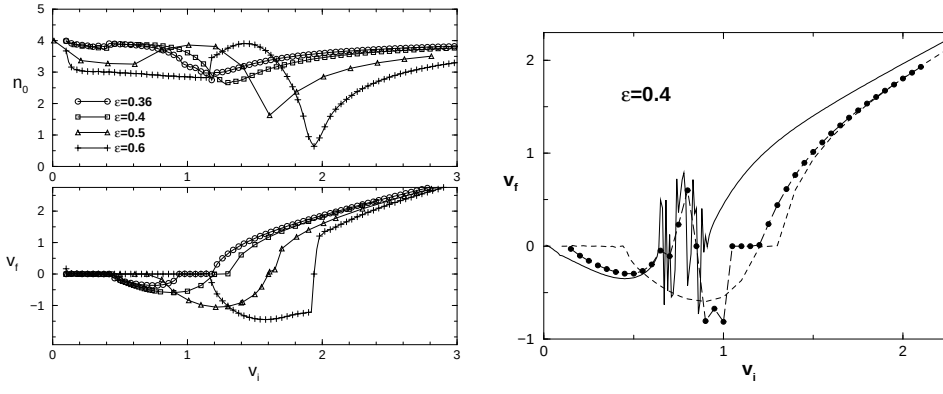

Fig. 7. On the left, we show numerical simulations of the full GP equation, showing the dependence of n_0, related to the number of atoms N (top frame), and final velocity v_f (bottom frame), with respect to the initial velocity v_i. The results of both frames are shown for different values of ε, as indicated inside the top frame. On the right, we show a comparison between variational and full numerical results for different values of ε. The initial value (for $v_i = 0$) $n_0 = 4$ can be rescaled as explained in the text. All the quantities are dimensionless. Obtained from Ref. 49.

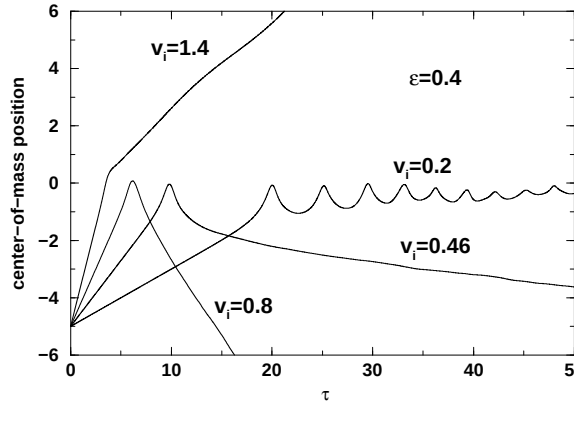

Fig. 8. For a fixed value of $\varepsilon = 0.4$, we present full numerical solution of the GP equation, with the time evolution of the center-of-mass position, considering different values of the initial velocity, as given inside the frame. The results, given for $n_0 = 4$, can be rescaled as explained in the text. All the quantities are dimensionless. Obtained from Ref. 49.

One can also observe, through the results given in the right frame of Fig. 7, that numerical simulations of the variational Eqs. (79)–(81) reproduce only qualitatively the behavior observed in the full numerical solution of the GP equation. In this figures, we observe the behavior of the final velocity as a function of the initial velocity, for $\varepsilon = 0.4$ and $n_0 = 4$. With a solid line we represent the variational results obtained from Eq. (79) and, with a dashed line, the full numerical solution. We note that the full numerical solution shows a window, between two trapped regions, where the soliton is reflected by the impurity. The variational result shows the window of reflection starting for smaller initial velocities and, instead of a

trapped region, a more complicated dynamics near the points where the regime of reflection starts or finishes. One can improve the variational approach by taking into account the influence of radiative friction on the soliton motion on the impurity as given in Ref. 61. The addition of a term $c\zeta^2\zeta_\tau$, where c is a phenomenological constant, in the second of Eqs. (79), has the effect of damping the oscillations ($\sim 1/\sqrt{\tau}$), improving the results as compared with full numerical solutions. By using $c = 0.01$, we can also observe the second trapped region close to the exact results (see the curve with solid circles in the right frame of Fig. 7).

The variational equation results, without the damping term, show a more complicated (probably chaotic) dynamics in the region where the reflection occurs. In this region, we also can see the more rare events with the transmission of soliton through the impurity. This observation resembles the phenomena observed at the interaction of the sine-Gordon equation kink with a local defect.[62] The system of ODEs (two-mode model) has a similar structure as Eqs. (79), showing chaotic behaviors, leading always to a finite time for the period of the soliton trapping. This phenomenon is due to stochastic instabilities inherent to this dynamical system. The reason for this phenomenon is that the finite dimensional system, like the one given by Eqs. (79), cannot take into account the soliton radiation that interacts with the defect. The effect of the radiation leads to the appearance of the damping in Eqs. (79) that changes the long-time behavior of the system. In particular, the radiative damping can lead to the long-time regular dynamics.[62] We should note that, in the present case of bright soliton propagation through a delta-like impurity, we have not faced the same kind of problem of applicability of the approach as the one observed in Ref. 52. As discussed before, the result was expected considering that in Ref. 52 the collective variables have to be modified due to the background evolution. We should add that we have used a modified variational approach including chirp, presenting additional degree of freedom. The impurity couples the internal degrees of freedom with the translational; so it occurs energy exchange between modes, such that we have reflection or transmission for the parameters where the effective particle method predict trapped regime.[55]

5.3. *Full numerical three-dimensional results*

In order to check the validity of the 1D reduction, in case of point-like nonlinear impurity, we have also performed full 3D numerical calculations. We have obtained numerically the ground-state solutions by solving the original 3D equation, Eq. (1), with the nonlinear cubic term multiplied by $1 + \varepsilon\delta(\zeta)$, and considering the trap only in the transversal directions.

The results are given in Fig. 9, for $2\pi n_0 = 5$ and 10, showing the ground-state behavior as a function of ζ, at the origin in the transversal directions. We observe that there is a critical value for the parameter ε of the nonlinearity such that for larger ε the system collapses. For example, in the case of $2\pi n_0 = 10$, the system collapses if we consider $\varepsilon \geq 0.45$. And, in the case of $2\pi n_0 = 5$, the

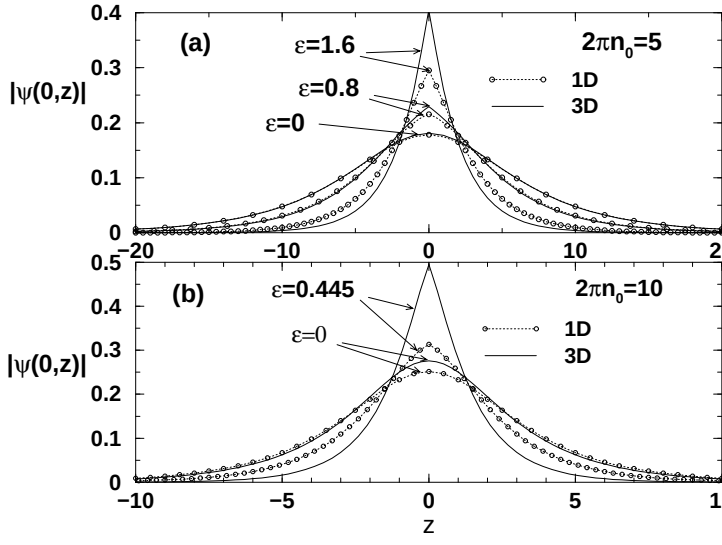

Fig. 9. In the above Figs. (a) and (b) we show results for the ground-state solutions obtained by solving the original 3D equation given in Eq. (1)(solid line) including impurity, in comparison with the corresponding 1D solutions (dashed-lines with dots), Eq. (95). All the quantities are in dimensionless units: $\zeta = z/l_\perp$, with $l_\perp \equiv \sqrt{\hbar/(m\omega_\perp)}$; and the wave-function is normalized to one, such that $|\psi(0,\zeta)|^2 \equiv |\Psi(\mathbf{r},t)||^2_{|\mathbf{r}|=z}(l_\perp^3/N)$. The parameter we have considered, n_0 and ε, are given inside the figures. Obtained from Ref. 49.

system collapses for $\varepsilon \geq 1.65$. The deviation from the analytical prediction, that one can observe particularly in the case of $2\pi n_0 = 10$, is connected with the fact that the contribution of the nonlinear term in the transverse direction becomes comparable with the transverse harmonic potential. So, as explained before, the 1D approximation is expected to be violated.

We found it illustrative to present in Fig. 10 the relation between the two critical limits: $k_\perp(\varepsilon) \equiv n_{0,\max}/4$ and the inhomogeneity parameter ε_c. When $\varepsilon = 0$ we have the well-known $k_\perp = N_c|a_{s0}|/l_\perp \approx 0.676$. As the parameter ε of a delta-like impurity increases, the corresponding negative value of the nonlinear term of Eq. (1) also increases, and the maximum number of atoms N_c will decrease (considering fixed a_{s0} and $l_\perp$). The agreement of 1D with 3D model was also verified in a dynamical calculation, using a specific example where the soliton is reflecting at the impurity. The results of the 3D dynamical calculation are shown in Fig. 10, considering the distance of the impurity from the origin to be $\Delta\zeta = 25$. In this case, we have considered parameters that correspond to the 1D parameters of Figs. 7 ($n_0 = 4$, $\varepsilon = 0.4$, $v_i = 0.8$). After proper rescaling [see Eq. (101)], with $n_0 = 5/(2\pi)$, we obtain $\varepsilon = 2$ and $v_i = 0.16$. We have presented several plots of the soliton profile using time steps such that $\Delta\tau = 50$. We observe the soliton reflecting at the impurity, following the same behavior as observed in the 1D numerical results. From an analysis of the critical limits given on the left side of Fig. 10, one should

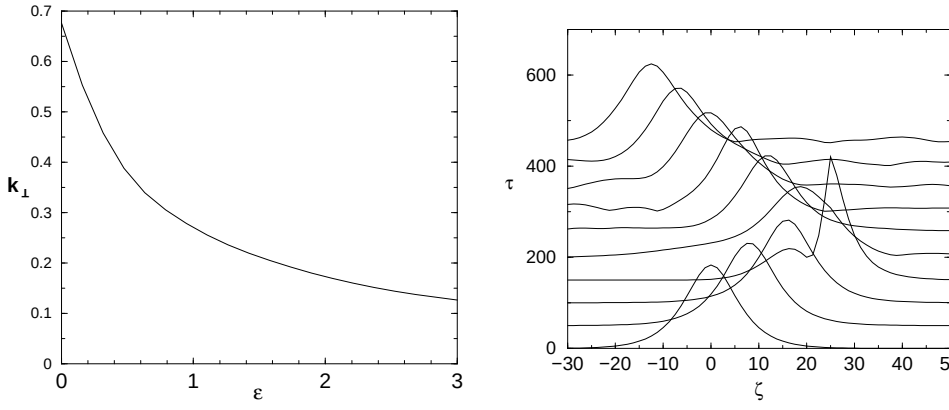

Fig. 10. On the left, we show a plot with the relation between the critical numbers $k_\perp$ and ε_c. The maximum number of atoms N_c is given by $k_\perp = N_c|a_{s0}|/l_\perp$, and ε is the impurity parameter for delta-like inhomogeneity. The curve shows the limit between two regions for the condensate: the lower part is the allowed region and the upper part is the collapsing region. Obtained from Ref. 49. On the right, we show the 3D numerical evolution of a soliton reflecting at an impurity placed at the position $\zeta = 25$, considering $2\pi n_0 = 5$, $v_i = 0.16$ and $\varepsilon = 2$, for the case of delta-like impurity. The magnitude of the wave function $\psi(0, \zeta)$ is in arbitrary scale, and all the quantities are in dimensionless units.

expect that for $\varepsilon > 1.6$ the system will collapse. However, the results on the left side of Fig. 10 are obtained for the ground-state in static calculations; the results on the right side of Fig. 10 shows that such critical limits can be increased in some extend when one considers a dynamical calculation with some initial velocity.

The present investigation of the local variation in space of the atomic scattering length shows that different regimes of the soliton interaction with the nonlinear impurity are possible. They are observed trapping, reflection and transmission regimes. The most interesting effect is the reflection of the atomic soliton by the attractive nonlinear impurity. We have also verified the occurrence of collapse of the soliton on the attractive impurity, when the strength of the impurity (or the initial number of atoms) exceeds a certain critical value, *even in true 1D*. This effect in 1D BEC resembles the collapsing phenomena that occur in 2D BEC. By using the time-dependent variational approach we obtain a good description of the collapsing phenomena and, qualitatively, the reflection and trapping dynamics. The usual 3D collapse of the ground state have a critical number of atoms reduced by increasing the strength of the impurity.

The present approach can be more easily implemented in optical induced Feshbach experiments, as discussed in Ref. 63, with optimistic perspectives of applications in current experiments with ultracold atoms. The physical parameters can be estimated by using the optical method for the variation of the scattering length.[63] By focusing a laser beam or using mask, we can define a region l_ε where the scattering length a_s is varying, as discussed in Sec. 3.2 for the case of a smooth varying inhomogeneity. In the experiments reported in Refs. 15 and 16 the characteristic

length is about 1.5μm, implying that $l_\varepsilon \geq 5\mu m$. For the case of a sudden variation of the two-body scattering length, represented by a nonlinear jump inhomogeneity, using analogy with a nonlinear optical problem,[55] we presented the condition for the multiple bright matter soliton generation.

5.4. *Bright solitons under time-dependent trap*

Let us consider the case when the longitudinal trap is time dependent, with $V = (1/2)\omega_0^2 f(\tau)\zeta^2$, and $f(\tau) = 1 + \varepsilon\cos(\Omega\tau)$. We can look for the solution in the form of chirped soliton, as given by Eq. (74). Applying the variational approach, we obtain the equation for the soliton width and coordinate

$$a_{\tau\tau} = \frac{16}{\pi a^3} - \frac{4n_0}{\pi^2 a^2} - 2f(\tau)\omega_0^2 a\,, \tag{102}$$

$$\eta_{\tau\tau} = -2f(\tau)\eta\,, \tag{103}$$

where $n_0 = 2A^2 a$. For the harmonic modulation of $f(\tau)$ the equation of motion for the center of soliton is the Mathieu equation. Thus, the parametric resonances in the soliton oscillations occur when

$$\Omega = \frac{2\sqrt{2}}{n}\,(n = 1, 2, 3, \ldots)\,. \tag{104}$$

It is possible for some set of parameters to have the same resonance in the oscillations of the width. Then a double parametric resonance in the oscillations of the center and the width of soliton appears.[64]

When the frequency of the trap is high $V \sim (1/\varepsilon)\alpha(\tau/\varepsilon)f(\zeta)$, $\varepsilon \sim 1/\Omega$, $\Omega \gg 1$, the resulting dynamics can be investigated using the averaging of the GP equation over rapid modulations.[65] According to averaging method, the field is represented as

$$u(\zeta, \tau) = U + \varepsilon u_1 + \varepsilon^2 u_2 + \cdots \tag{105}$$

For the slowly varying field $V = \sqrt{1 + \varepsilon^2 f^2(\zeta)/2}\; U$ we obtain the averaged GP equation

$$iV_\tau + V_{\zeta\zeta} + 2|V|^2 V = \left[\alpha_0 f(\zeta) + \frac{\varepsilon^2}{2}\,(f_\zeta(\zeta))^2\right] V + O(\varepsilon^4)\,. \tag{106}$$

Thus the averaged dynamics is described as under the effective potential

$$W = \alpha_0 f(\zeta) + \frac{\varepsilon^2}{2}(f_\zeta(\zeta))^2\,. \tag{107}$$

This result shows, that we can manage the form of the trap potential via the rapid modulation in time of parameters.

For example when the time-dependent potential is

$$V(\zeta) = (-\alpha_0 + \alpha_1 \sin(\Omega t))f(\zeta),\; f(\zeta) = \zeta^2\,, \tag{108}$$

the averaged potential is

$$W = \left(-\alpha_0 + 2\,\frac{\alpha_1^2}{\Omega^2}\right)\zeta^2\,. \tag{109}$$

Thus when $\alpha_1 > \sqrt{|\alpha|/2}\Omega$, the sign of the effective potential is reversed and the solitary wave becomes stable. The analysis of the more complicated potentials can be found in Ref. 65.

5.5. *Adiabatic compression of soliton matter waves*

The *adiabatic* variations of the atomic scattering length in space can be used as an effective way for controlling soliton's parameters and to induce changes in their shape which could be useful for applications.[66] In contrast to abrupt variations, considered in the previous subsection, adiabatic changes make it possible to preserve the integrity of the soliton (no splitting occurs), this leading bright solitons to the compression of the pulse with the increase of the matter density. These phenomena are shown to exist both in the presence and in the absence of a parabolic confining potential. We find that, for bright solitons, except for the oscillatory motion around the bottom of the trap, the phenomena of pulse compression is practically the same as in the absence of the trap (this is particularly true for solitons initially at rest in the bottom of the trap). The possibility to compress BEC solitons could be an experimental tool to investigate the range of validity of the 1D GPE. Since the quasi one-dimensional regime is valid for low densities, it would be indeed interesting to see how far one can compress a soliton in a real experiment by means of adiabatic changes of the scattering length. In contrast with Josephson junctions and optical fibers, which require structural changes or preparation of new samples, the study of adiabatic nonlinear perturbations on BEC solitons appears more natural and easy to perform, since the strength of the nonlinear interaction can be changed by using only external fields. We also remark that soliton dynamics in a quasi one-dimensional BEC under time-dependent *linear* potential was recently studied in Ref. 67.

In order to model an adiabatic variation of the atomic scattering in 1D (cigar-shaped) BEC, we consider the following normalized Gross–Pitaevskii equation[20,68]

$$iu_\tau + u_{\zeta\zeta} + \sigma\gamma(\zeta,\tau)|u|^2u - \omega^2\zeta^2u = 0\,, \tag{110}$$

where u is the ground state wave function of the condensate, $\gamma(\zeta,\tau)$ is a slowly varying function of space and time, $\sigma \pm 1$ corresponds to the case of negative and positive scattering length a_s (ω denotes the longitudinal frequency of the trap).

Although the analysis can be performed for generic smooth functions $\gamma(\zeta,\tau)$, we shall restrict to the limiting case variation in the space: $\gamma \equiv \gamma(\zeta)$, being experimentally easier to realize. We will use the perturbative approach. Using the transformation $v = \sqrt{\gamma(\zeta)}u$ in Eq. (110), we have

$$iv_\tau + v_{\zeta\zeta} + \sigma|v|^2v = R(v)\,. \tag{111}$$

$R(v)$ is a small perturbation, since $L/L_\gamma \ll 1$, where L is the characteristic solitonic scale and L_γ is the scale of the scattering length modulation. We are also neglecting the terms $\gamma_{\zeta\zeta}/(2\gamma)v - (3/4)(\gamma_\zeta)^2 v/\gamma^2$ which are of the order L^2/L_γ^2. So, if we ignore the trap and the terms that are much smaller than the corresponding temporal and spatial characteristic scales, then

$$R(v) \simeq F(\zeta) v_\zeta\,, \quad \text{with} \quad F(\zeta) \equiv (\ln \gamma(\zeta))_\zeta\,. \tag{112}$$

With the initial condition as a single soliton,

$$v(\zeta,\tau) = \sqrt{2} A(\tau)\,\mathrm{sech}[A(\tau)(\zeta - \eta(\tau))]\,\exp[\mathrm{i}(k(\tau) + C(\tau)((\zeta - \eta(\tau)))]\,, \tag{113}$$

then, with the norm equation $N = \int |v|^2 d\zeta$, we find $A = A_0\gamma(\tau)$. So, for the amplitude and the width of the soliton, we have $A_\psi = A_0\sqrt{\gamma}$, $a = 1/(A_0\gamma)$, in agreement with the variational approach. From this, we conclude that an adiabatic increase of the scattering length can be used to narrow the width of a bright soliton matter wave. Soliton compression phenomena induced by linear damping amplification are also known from nonlinear optics.[69]

Following soliton theory of Refs. 70 and 71,

$$\begin{aligned} A_\tau &= \int_{-\infty}^{\infty} \mathrm{sech}(y)\,\mathrm{Im}(R) dy\,, \\ C_\tau &= \int_{-\infty}^{\infty} \tanh(y)\,\mathrm{sech}(y)\,\mathrm{Re}(R) dy\,, \\ \eta_\tau &= 2\sigma C + \frac{1}{A^2}\int_{-\infty}^{\infty} y\,\mathrm{sech}(y)\,\mathrm{Im}(R) dy\,, \end{aligned} \tag{114}$$

we find that the equations for the soliton's parameters (113) are:

$$\begin{aligned} A_\tau &= AC\int_{-\infty}^{\infty} F\left(\frac{y}{A} + \zeta\right)\mathrm{sech}^2(y) dy \approx 2ACF(\zeta)\,, \\ C_\tau &= A^2\int_{-\infty}^{\infty} F\left(\frac{y}{A} + \zeta\right)(\mathrm{sech}^2(y) - \mathrm{sech}^4(y)) dy \approx \frac{2}{3}A^2 F(\zeta)\,, \\ \eta_\tau &= 2C + \frac{C}{A}\int_{-\infty}^{\infty} F\left(\frac{y}{A} + \zeta\right) y\,\mathrm{sech}^2(y) dy \approx 2C(1 + O(1/L^2))\,. \end{aligned} \tag{115}$$

From these equations it follows that $(F(-\infty) = 1)$

$$A = A_0\gamma(\zeta), C_{fin} = \sqrt{C_{in}^2 + \frac{1}{3}A_0^2(\gamma^2(\zeta) - \gamma_{ini}^2)}\,, \tag{116}$$

where the subscripts *ini* and *fin* correspond respectively to the initial and final values for C and γ.

We shall compare these predictions with direct numerical integrations of Eq. (110). In Fig. 11 the amplitude of a bright soliton as a function of the position of the center of mass is plotted for the case of a space dependent variation of the scattering length in the absence of the parabolic trap. The soliton, initially

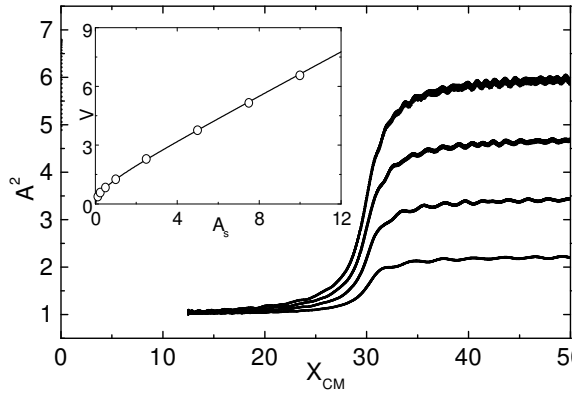

Fig. 11. The squared amplitude of a bright soliton vs center of mass position for different values of the amplitude A_s of a kink-like spatial inhomogeneity centered at ζ =30, given by Eq. (116). The curves, from bottom to top, refer to $A_s = 2.5$, 5.0, 7.5, 10.0, respectively. The other parameters are $s = 0.2$, $T_f = 60$, $\sigma = 1$, $A_0 = 1$. The soliton is initially at rest, placed at position $\zeta_{ini} = 12.5$. In the inset we show the soliton final velocity as a function of A_s. The open dots are numerical values while the continuous curve is obtained from Eqs. (115) and (116) as $V_{fin} = \frac{A_0}{\sqrt{3}}\sqrt{\gamma_{fin}^2 - \gamma_{in}^2}$. Obtained from Ref. 66.

at rest, is sucked into the higher scattering length region, and reaches a constant velocity after passing the inhomogeneity. Also, in this case, there is an excellent agreement with variational analysis (see the inset of Fig. 11).

The dynamics of matter wave solitons in the presence of a spatially varying atomic scattering length is also considered in Ref. 72. Using the adiabatic perturbation theory for solitons, the authors have derived the effective equation of motion of the soliton center of mass η for the variation $a_s = a_0 + a_1\zeta$ and so $\gamma(\zeta) = 1 + \delta\zeta$, namely:

$$\eta_{\tau\tau} = -V_\eta + \frac{A^2(0)}{6\gamma^2(0)}\left(\frac{\partial\gamma^2}{\partial\eta}\right), \tag{117}$$

where

$$V(\eta) = \frac{1}{2}w_b^2\eta^2 - \beta\eta\,, \qquad \beta = \frac{A^2(0)\delta}{3(1+\delta\eta(0))^2}\,, \qquad \omega_b = \sqrt{\omega_0^2 - \delta\beta}\,. \tag{118}$$

Such form of a variation leads to an effective gravitational potential influencing on the motion of the fundamental soliton. Also the oscillations frequency in the trap is modified.

5.6. *Bright soliton under time-dependent scattering length*

The resonant dynamics of the chirped matter wave soliton under oscillating in time scattering length are considered in Refs. 73 and 74. Using the variational approach with the Gaussian ansatz for the wavefunction, we obtain the equation for the

soliton width

$$a_{\tau\tau} = \frac{1}{a^3} - \frac{\gamma(\tau)}{a^2} - f(\tau)a\,. \tag{119}$$

When the trap is absent, the dynamics can be analyzed in detail since we have dealt with the periodically perturbed Kepler problem. Using the action-angle variables we can find the condition of the nonlinear resonance in the chirped soliton oscillations.

For nonlinearity management,[74] we introduce the small parameter $\varepsilon = \omega_z/\Omega$ and assume that the nonlinear management amplitude is large compared to the averaged value. We write accordingly

$$\gamma(\tau) = \gamma_0 + \frac{\gamma_1}{\varepsilon}\,\sin\left(\frac{\tau}{\varepsilon}\right), \tag{120}$$

and perform the asymptotic analysis following the Kapitsa averaging theorem. Expanding $a(\tau) = a_0(\tau) + \varepsilon a_1(\tau, \tau/\varepsilon) + \cdots$ and substituting this form into Eq. (119) we get a compatibility condition which reads

$$a_{0,\tau\tau} = \frac{1}{a_0^3} - a_0 + \frac{\gamma_0}{a_0^2} + \frac{\gamma_1^2}{a_0^5}\,. \tag{121}$$

The initial conditions are: $a_0(0) = a(0)$, $a_0'(0) = a'(0) - \gamma_1/a_0^2$.

Let us first deal with $\gamma_0 = 0$. If $|\gamma_1| \le \gamma_c$, $\gamma_c = (4/27)^{1/4} \approx 0.62$, then Eq. (121) admits a unique fixed point describing the width of the ground state

$$a_g^2 = \frac{2}{\sqrt{3}}\,\cos\left[\frac{1}{3}\arccos\left(\frac{\gamma_1^2}{\gamma_c^2}\right)\right]. \tag{122}$$

If $|\gamma| > \gamma_c$, then

$$a_g^2 = \left(\frac{\gamma_1^2}{2}\right)^{1/3}\left[\left(1+\sqrt{1-\frac{\gamma_1^4}{\gamma_c^4}}\right)^{1/3} + \left(1-\sqrt{1-\frac{\gamma_1^4}{\gamma_c^4}}\right)^{1/3}\right], \tag{123}$$

and a_g increases with γ_1 and goes from the value 1 for $\gamma_1 = 0$ to the asymptotic value $a_g \sim \gamma_1^{2/3}$ for large γ_1. The linear stability analysis of Eq. (121) shows that the fixed point is stable. The width oscillates near this value with the frequency $\omega_s = \sqrt{6 - 2/a_g^4}$. In the general case $\gamma_0 \neq 0$, $\gamma_1 \neq 0$, there exists a unique fixed point which is the unique positive zero of the equation $a^2 - a^6 + \gamma_0 a^3 + \gamma_1^2 = 0$.

Influence of the random modulations of the nonlinearity on the evolution of chirped soliton has been considered in Ref. 75. The soliton's distortion time has been calculated.

In Ref. 76 the dynamics of the bright soliton in the BEC with time-dependent atomic scattering length in an expulsive potential $\omega_0^2 < 0$ has been studied. Using the Darboux method the family of exact solutions was found, which shows, that the bright soliton can be compressed to high local matter densities by increasing the absolute value of atomic scattering length. The seed solution has been taken as the modulationally unstable plane wave solution. So the soliton was the bright

soliton embedded into the background. Previously such solutions has been discussed intensively in the nonlinear optics (see Refs. 77 and 78).

5.7. *Soliton-soliton and N-solitons interaction in the trap potential*

The soliton-soliton interaction in the trap can be studied using the perturbation theory based on the inverse scattering transform.[79] Let us look for the solution of the form of two well separated solitons; i.e., when the relative distance between them is much more than that of the soliton widths $a_i = 1/(2\nu_i)$, $i = 1, 2$.

$$u(x,t) = u_1(x,t) + u_2(x,t) \tag{124}$$

where the single soliton solution is

$$u_n(x,t) = 2\nu_n \operatorname{sech}[2\nu_n(x-\xi_n)]e^{i2\mu_n(x-\xi_n)+i\delta_n} \tag{125}$$

with $n = 1, 2$. Then, the Lagrangian can be represented as

$$\begin{aligned}\mathcal{L} = \sum_{n=1,2}\left[\frac{i}{2}(u_{n,t}u_n^* - c.c.) - \frac{1}{2}|u_{n,x}|^2 + \frac{1}{2}|u_n|^4 - \frac{1}{2}\omega^2 x^2|u_n|^2\right] \\ - i\varepsilon(u_1^* R_{21}[u_1] + u_2^* R_{12}[u_2] + c.c.)\,,\end{aligned} \tag{126}$$

where

$$\varepsilon R_{mn}[u_n] = i(u_m^* u_n^2 + 2u_m|u_n|^2)\,, \tag{127}$$

with $m, n = 1, 2$, $m \neq n$. And we must neglect u_n dependence in R_{mn} when taking the variational derivative.

Next we apply the variational approach[50] to the Lagrangian

$$L = \int_{-\infty}^{+\infty} \mathcal{L}(x,t)dx\,, \tag{128}$$

where $\mathcal{L}$ is given by Eq. (126). From Eqs. (125), (126) and (128), we obtain

$$\begin{aligned}L = \sum_{n=1,2}\left[8\nu_n\mu_n\xi_{n,t} - 4\nu_n\delta_{n,t} - \frac{8\nu_n^3}{3} - 8\nu_n\mu_n^2 + \frac{16}{3}\nu_n^3 - 2\omega^2\left(\frac{\pi^2}{48\nu_n} + \nu_n\xi_n^2\right)\right] \\ + 96\nu_1^2\nu_2\,\exp(-2\nu r) + 96\nu_1\nu_2^2\,\exp(-2\nu r)\,.\end{aligned} \tag{129}$$

Using the Euler–Lagrange equations

$$\frac{\partial L}{\partial \eta_i} - \frac{d}{dt}\frac{\partial L}{\partial \eta_{i,t}} = 0\,, \tag{130}$$

where η_i are the eight parameters $\nu_{1,2}$, $\mu_{1,2}$, $\delta_{1,2}$ and $\xi_{1,2}$, we find the evolution equations for the soliton parameters

$$\frac{d\nu_n}{dt} = (-1)^n 16\nu^3 e^{-2\nu r}\,\sin(\phi)\,, \tag{131}$$

$$\frac{d\mu_n}{dt} = -\frac{1}{2}\omega^2\xi_n + (-1)^n 16\nu^3 e^{-2\nu r}\,\cos(\phi)\,, \tag{132}$$

$$\frac{d\xi_n}{dt} = 2\mu_n + 4\nu e^{-2\nu r}\,\sin(\phi)\,, \tag{133}$$

$$\frac{d\delta_n}{dt} = -\frac{1}{2}\omega^2\left(\xi_n^2 - \frac{\pi^2}{48\nu_n^2}\right) + 2(\nu_n^2+\mu_n^2) + 8\mu\nu e^{-2\nu r}\,\sin(\phi) + 24\nu^2 e^{-2\nu r}\,\cos(\phi)\,, \tag{134}$$

where $\phi = 2\mu r + \psi$, $\nu = (\nu_1+\nu_2)/2$, $\mu = (\mu_1+\mu_2)/2$, $r = \xi_1 - \xi_2$, $\psi = \delta_2 - \delta_1$. Here r is the distance between the solitons and ψ is their relative phase. It was assumed that $r > 0$ and $|\nu_1 - \nu_2| \ll \nu$, $|\mu_1 - \mu_2| \ll \mu$, $|\nu_1 - \nu_2| r \ll 1$ and $\nu r \gg 1$. From this system we obtain the equation for the relative distance

$$\frac{d^2 r}{dt^2} = -\omega^2(t) r - 64\nu^3 e^{-2\nu|r|}\,\mathrm{sgn}(r)\,\cos(\phi)\,, \tag{135}$$

where $\mathrm{sgn}(r) = 1$, $r > 0$, $= -1$, $r < 0$. In dimensional units it has the form

$$\frac{d^2\bar{r}}{d\bar{t}^2} = -\omega_x^2(t)\bar{r} - 64 a_\perp \omega_\perp^2 \nu^3 e^{-2\nu|\bar{r}|/a_\perp}\,\mathrm{sgn}(r)\,\cos(\phi)\,, \tag{136}$$

where $\nu = N|a_s|/(2a_\perp)$. This is the equation of motion of a unit mass particle in anharmonic effective potential

$$U(r) = \frac{1}{2}\omega^2(t) r^2 - 32\nu^2 e^{-2\nu|r|}\,\cos(\phi)\,. \tag{137}$$

Since the perturbation of trap is small $\omega_0^2 \ll 1$, the equation for the relative phase can be written as

$$\frac{d^2\phi}{dt^2} = 128\nu^4 e^{-2\nu|r|}\,\sin(\phi)\,. \tag{138}$$

An inspection of the potential given in Eq. (137) shows that the solitons with the relative phase $\phi = 0$ ($\phi = \pi$) have attractive (repulsive) interaction. When $\phi = \pi$ and $\omega^2(t) = \omega_0^2$, as we can see from the expression for the effective potential, the minimum occurs for r at some equilibrium distance r_e. It corresponds to the stable bisoliton.[39] The parametric resonance in the soliton-soliton interactions considered recently in Ref. 79. The similar effect stable multisoliton occurs for N-solitons with π phase difference between neighbor solitons in the trap potential.[46]

6. Bright Solitons in Dense Condensate in Cigar-Shaped Trap

Now we shall consider dynamics of BEC in the cigar-shaped trap by means of a variational approach without assumption that the field variables change slowly along the trap axis (see Ref. 23) when the condition (15) is not fulfilled. To this end, we approximate the wave function as

$$\psi = \frac{1}{\sqrt{\pi}b(z,t)}\,\exp\left(-\frac{r^2}{2b^2(z,t)}\right)\exp\left(\frac{i}{2}\alpha(z,t)r^2\right)\Psi(z,t)\,. \tag{139}$$

Here $b(z,t)$ characterizes the local radius of the condensate and $\alpha(z,t)r$ gives the local radial velocity. Substitution of Eq. (139) into Eq. (11) and the result into the wave function (10) with integration over the radial coordinate yield an effective 1D Lagrangian

$$\begin{aligned}\mathcal{L}_{1D} = {} & \frac{i\hbar}{2}\left(\Psi\Psi_t^* - \Psi^*\Psi_t\right) + \frac{\hbar^2}{2m}|\Psi_z|^2 + \frac{1}{2}m\omega_\perp^2 b^2|\Psi|^2 \\ & + V(z)|\Psi|^2 + \frac{g}{4\pi b^2}|\Psi|^4 + \frac{\hbar}{2}\alpha_t b^2|\Psi|^2 \\ & + \frac{\hbar^2}{2m}\left[\left(\frac{1}{b^2} + \alpha^2 b^2 + \frac{b_z^2}{b^2} + \frac{1}{2}\alpha_z^2 b^4\right)|\Psi|^2 + \frac{i}{2}\alpha_z b^2(\Psi\Psi_z^* - \Psi^*\Psi_z)\right]. \end{aligned} \tag{140}$$

To simplify the notation, we introduce dimensionless variables:

$$\begin{gathered}\tau = \omega_\perp t\,, \qquad z = a_\perp \zeta\,, \qquad \Psi = \frac{u}{\sqrt{l_\perp}}\,, \qquad b = l_\perp w\,, \\ \alpha = \frac{\beta}{l_\perp^2}\,, \qquad G = \tfrac{a_s}{l_\perp}\,. \end{gathered} \tag{141}$$

In the these variables the 1D Lagrangian becomes

$$\begin{aligned}\mathcal{L}_{1D} = \frac{\hbar^2}{m l_\perp^3}\Bigg[& \frac{i}{2}(uu_\tau^* - u^*u_\tau) + \frac{1}{2}|u_\zeta|^2 + \frac{1}{2}w^2|u|^2 + V(\zeta)|u|^2 \\ & + G\frac{|u|^4}{w^2} + \frac{1}{2}\beta_\tau w^2|u|^2 + \frac{1}{2}(w^{-2} + \beta^2 w^2 + w_\zeta^2 w^{-2} \\ & + \frac{1}{2}\beta_\zeta^2 w^4)|u|^2 + \frac{i}{4}\beta_\zeta w^2(uu_\zeta^* - u^*u_\zeta)\Bigg]. \end{aligned} \tag{142}$$

Thus, in the above reduction, the evolution of BEC is described by the complex longitudinal wave function $u(\zeta,\tau)$ and two real functions, $w(\zeta,\tau)$ and $\beta(\zeta,\tau)$, corresponding to the local mean radius of the condensate and its radial velocity, respectively. Equations governing the evolution of these variables are to be obtained from the action principle

$$S = \int L dt = \min, \qquad L = \int \mathcal{L}_{1D} d\zeta \tag{143}$$

with the effective Lagrangian density given by Eq. (142). We have:

$$\begin{aligned} & iu_\tau + \frac{1}{2}u_{\zeta\zeta} - V(\zeta)u - 3G\frac{|u|^2 u}{w^2} \\ & \quad -\frac{1}{2}\left[\frac{2}{w^2} + \frac{w_{\zeta\zeta}}{w} + \left(\frac{w_\zeta}{w} - \frac{i}{2}\beta_\zeta w^2\right)\frac{(|u|^2)_\zeta}{|u|^2}\right. \\ & \quad \left. -\frac{1}{2}\beta_\zeta^2 w^4 - \frac{i}{2}\beta_{\zeta\zeta}w^2 - i\beta_\zeta w w_\zeta\right] = 0\,, \end{aligned} \tag{144}$$

$$(w^2|u|^2)_\tau + \left[\frac{i}{2}w^2(uu_\zeta^* - u^*u_\zeta) + w^4|u|^2\beta_\zeta\right]_\zeta = 2\beta w^2|u|^2\,, \tag{145}$$

$$\beta_\tau = \frac{w_{\zeta\zeta}}{w^3} + \frac{1-w_\zeta^2}{w^4} + \frac{w_\zeta}{w^3}\frac{(|u|^2)_\zeta}{|u|^2} - 1 - \beta^2 - \beta_\zeta^2 w^2 + \frac{i(u_\zeta u^* - uu_\zeta^*)}{2|u|^2}\beta_\zeta + 2G\frac{|u|^2}{w^4}\,, \tag{146}$$

where the longitudinal wave function is normalized as follows

$$\int |u|^2 d\zeta = N\,. \tag{147}$$

Thus, we have transformed the 3D GP equation to a quasi-1D form for the case of elongated cigar-shaped geometry when the radial distributions of the condensate density and its radial velocity can be approximated by simple Gaussian functions. The variables in Eqs. (144)–(146) depend only on one spatial coordinate — a strong advantage in numerical simulations. Besides that, systems (144)–(146) can be analyzed analytically in some important limiting cases.

In a stationary state all velocities are equal to zero ($v = 0$, $\beta = 0$), density ρ does not depend on τ and the condensate wave function $u(\zeta,\tau)$ depends on τ only through the phase factor $\exp(-i\mu\tau)$, where μ is dimensionless chemical potential. Setting $\beta = 0$ and introducing the stationary variables $U(\zeta)$ and $\sigma(\zeta)$ by the formulae

$$u(\zeta,\tau) = e^{-i\mu\tau}U(\zeta)\,, \qquad w^2(\zeta,\tau) = 1/\sigma(\zeta)\,, \tag{148}$$

after some simple algebra we obtain from Eqs. (144)–(146) the following system

$$U_{\zeta\zeta} + \left(2\mu - 2V(\zeta) - \sigma - \frac{1}{\sigma} - \frac{\sigma_\zeta^2}{4\sigma^2}\right)U - 4G\sigma U^3 = 0\,, \tag{149}$$

$$\frac{1}{2}\left(\frac{\sigma_\zeta U^2}{\sigma}\right)_\zeta - \left(\sigma - \frac{1}{\sigma}\right)U^2 - 2G\sigma U^4 = 0\,. \tag{150}$$

Systems (149)–(150) has the energy functional

$$\mathcal{E} = \int \left[\frac{1}{2}U_\zeta^2 + V(\zeta)U^2 + G\sigma U^4 + \frac{1}{2}\left(\sigma + \frac{1}{\sigma} + \frac{\sigma_\zeta^2}{4\sigma^2}\right)U^2 - \mu U^2\right]d\zeta\,. \tag{151}$$

Here integrand can be considered as a Lagrangian with the spatial variable ζ playing the role of time.

First of all let us consider the limit of a low density BEC:

$$|G|U^2 \ll 1\,. \tag{152}$$

In the dimensional variables, with account of the estimate $U^2 \sim |\Psi|^2 l_\perp \sim n_1 l_\perp$ (where n_1 is the longitudinal density of the condensate), condition (152) coincides with the condition (15). Since the characteristic length in the axial direction cannot

be less than unity (i.e. $l_\perp$ in the dimensional units), from Eq. (150) we find in this limit

$$\sigma = 1 + \sigma_1\,, \qquad |\sigma_1| \sim |G|U^2 \ll 1\,. \tag{153}$$

Taking estimate (153) into account, we reduce Eq. (149) to the standard (stationary) 1D NLS equation

$$U_{\zeta\zeta} + 2(\mu - 1 - V(\zeta))U - 4GU^3 = 0\,. \tag{154}$$

This equation leads to well-known soliton solutions on the NLS equation

$$U(\zeta) = \frac{U_0}{\cosh(U_0\sqrt{2|G|}\,\zeta)}\,, \tag{155}$$

where U_0 is the amplitude of the soliton connected with the number of atoms $N = \int U^2 d\zeta$ by the relation

$$N = U_0\sqrt{\frac{2}{|G|}}\,, \tag{156}$$

and $\mu' = \mu - 1 = -|G|U_0^2$. Then condition (152) of applicability of the NLS equation can be written in the form [see (15)]

$$|\mu'| = |G|U_0^2 \sim (|G|N)^2 \ll 1\,. \tag{157}$$

It is clear that this condition breaks down for large enough number of atoms $N \sim 1/|G|$ and one cannot neglect the effect of the atomic interaction on the transverse size of BEC. The transverse degrees of freedom lead to the collapse instability of BEC (see e.g. Ref. 10), which, as is known, also takes place in BEC confined in a cigar-shaped trap. Numerical results of Refs. 20 and 22 indicate that BEC in the cigar-shaped trap collapses for

$$|G|N > 0.676 \tag{158}$$

and in this region of parameters the soliton solution ceases to exist. Our quasi-1D approach captures this essential property of the attractive BEC, and hence, in our approach, the bright soliton solution can be studied in the whole region of its existence.

We have solved numerically the systems (149) and (150) with $G < 0$ and $V = 0$ under the boundary conditions

$$U(\zeta) \to 0 \quad \text{at} \quad \zeta \to \pm\infty\,. \tag{159}$$

In Fig. 12 we show the wave function amplitude and transverse radius profiles of BEC for several values of $|G|N$. It is clearly seen that the amplitude of the soliton increases while its transverse radius decreases with growth of $|G|N$. For small $|G|N$ the solution is well approximated by the NLS solution (155), especially the amplitude profile. At $\zeta \to \pm\infty$ the radius approaches 1. What corresponds to the small amplitude limit when the transverse wave function is given by the oscillator

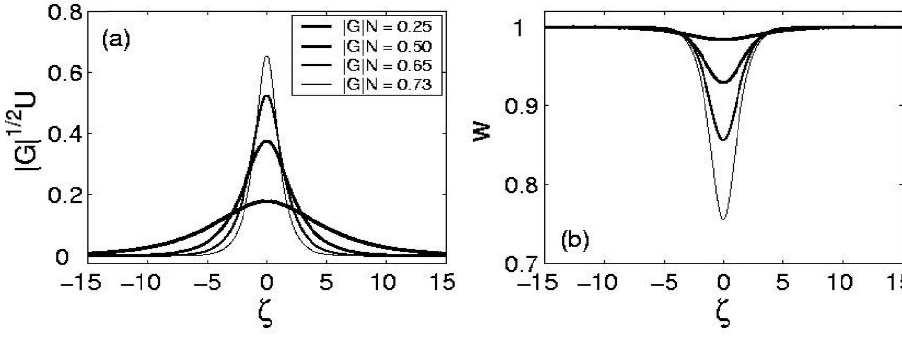

Fig. 12. Wavefunction amplitude and transverse radius (W) profiles of BEC for several values of $|G|N$, as given in the left frame.

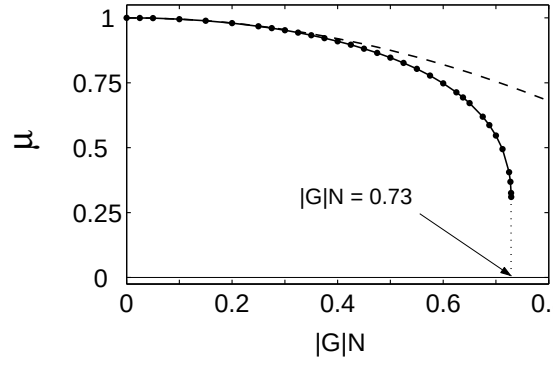

Fig. 13. The dependence of μ on $|G|N$ in quasi-1D approximation (solid line) and in the NLS equation case (dashed line).

ground state. A fast decrease of w in the center of the soliton with growth of $|G|N$ precedes the collapse instability of BEC.

To clarify the transition to collapse, we show the dependence of μ on $|G|N$ in the presented quasi-1D approximation (the solid line) and in the NLS equation case (the dashed line) in Fig. 13. We see that $\partial N/\partial\mu$ vanishes at $|G|N \cong 0.73$, which is in reasonably good agreement with the exact 3D critical value given by (158).

Finally, the axial width of this soliton solution is about unity (i.e. $\sim l_\perp$ in the dimensional units) in qualitative agreement with the features of bright solitons observed experimentally in Refs. 15 and 16.

7. Reduction of Gross–Pitaevskii Equation in Pancake-Type Trap to 2D NLS Equation

Let us consider the case of tight trap in z-direction, so $\omega_z \gg \omega_\perp$ and $s_\parallel^2 \ll l_\perp^2$. We assume that the quantum pressure in z-direction much larger than a nonlinear

interaction, i.e.

$$\frac{\hbar^2}{2ms_\parallel^2} \gg g|\psi|^2, |\psi|^2 \sim \frac{N}{2\pi l_\perp^2 s_\parallel}\,, \tag{160}$$

where $s_\parallel$ ($\sim l_\parallel$) is the condensate size in z-direction. Note that $l_\perp \neq s_\perp$ because the transverse size of the condensate is determined by the attractive interaction between atoms and not by the trap potential. Then we have the condition

$$\frac{N|a_s|l_\parallel}{s_\perp^2} \ll 1\,, \tag{161}$$

which means that the longitudinal motion is reduced to zero quantum oscillations.

We represent the condensate wave function in the form

$$\psi = \Phi(x, y; t)R(z)\,, \tag{162}$$

where $R(z)$ is the ground state wave function of the axial motion of atoms,

$$R(z) = \frac{1}{\pi^{1/4} l_\parallel^{1/2}} \exp\left(-\frac{z^2}{2l_\parallel^2}\right). \tag{163}$$

As in Sec. 2, we obtain the equation for the transverse wave function Φ

$$i\hbar\Phi_t = -\frac{\hbar^2}{2m}\nabla_\perp^2\Phi + \frac{m\omega_\perp^2}{2} r_\perp^2\Phi + g_{2D}|\Phi|^2\Phi\,, \tag{164}$$

with $g_{2D} = g\sqrt{2}\pi l_\parallel$. The condensate size can be estimated from the Hamiltonian

$$H = \int d^2r \left[\frac{\hbar^2}{2m}|\nabla\Phi|^2 + \frac{m\omega^2 r^2}{2}|\Phi|^2 - \frac{g_{2D}}{2}|\Phi|^4\right]. \tag{165}$$

It can be approximated by the order of magnitude as

$$H \sim \frac{\hbar^2 N}{ms_\perp^2} + m\omega^2 N s_\perp^2 + \frac{g_{2D}N^2}{s_\perp^2}\,. \tag{166}$$

The minimization with respect to $s_\perp$ gives

$$s_\perp \sim l_\perp \left(1 - \frac{|a_s|N}{l_\parallel}\right)^{1/4}. \tag{167}$$

Thus we can conclude that the condensate exists for $N < N_c \sim l_\parallel/|a_s|$. Using the inequality (161) we obtain that the parameters should satisfy the condition

$$\frac{N|a_s|l_\parallel}{l_\perp^2}\left(1 - \frac{N|a_s|}{l_\parallel}\right)^{-1/2} \ll 1\,. \tag{168}$$

The dimensionless form of Eq. (164) can be obtained by the change of variables

$$\tau = t\omega_\perp\,, \qquad \rho = \frac{\sqrt{2}r_\perp}{l_\perp}\,, \qquad u = \sqrt{\frac{|g_{2D}|}{\hbar\omega_\perp}}\Phi\,. \tag{169}$$

Thus we arrive at the dimensionless 2D GP equation

$$iu_\tau = -\nabla_\perp^2 u + \frac{1}{4}\rho^2 u + \sigma|u|^2 u, \sigma = \pm 1\,. \tag{170}$$

8. Stable Bright Solitons in Multidimensional Condensate. Nonlinearity Management.

The coefficient in front of the cubic term of the Gross–Pitaevskii equation (1), proportional to the scattering length, may be both positive and negative, which corresponds, respectively, to repulsive and attractive interactions between the atoms. In the case of an attractive interaction, a soliton may be formed in an effectively one-dimensional (1D) condensate;[15,16] however, in 2D and 3D cases the attraction results in the collapse of the condensate (*weak* and *strong* collapse, respectively[80]) if the number of atoms exceeds a critical value.

Recently developed experimental techniques[81] make it possible to effectively control the sign of the scattering length using an external magnetic field because the interaction constant can be changed through the Feshbach resonance.[82] This technique makes it possible to quickly reverse (in time) the sign of the interaction from repulsion to attraction, which gives rise, via the onset of collapse, to an abrupt shrinking of the condensate, followed by a burst of emitted atoms and the formation of a stable residual condensate.[81]

A natural generalization of this approach for controlling the strength and sign of the interaction between atoms and, thus, the coefficient in front of the cubic term, is the application of a magnetic field resonantly coupled to the atoms. In the general case, it consists of constant (*dc*) and time-dependent (*ac*) components. The dynamical behavior of 2D and 3D condensates in this case is then an issue of straightforward physical interest, as it may be readily implemented in experiments. This is the subject of the present section.[83]

It is noteworthy that, in the 2D case, this issue is similar to a problem which was recently considered in nonlinear optics for (2+1)D spatial solitons (i.e., self-confined cylindrical light beams) propagating across a nonlinear bulk medium with a layered structure, so that the size[84] and, possibly, the sign[85] of the Kerr (nonlinear) coefficient are subject to a periodic variation along the propagation distance (it plays the role of the evolutional variable, instead of time, in the description of optical spatial solitons). The same optical model also makes sense in the (3+1)D case, because it applies to the propagation of "light bullets" (3D spatiotemporal solitons[86]) through the layered medium.[85] Previously, a quasi-1D model was considered in which the BEC stability was affected by a rapid temporal modulation applied to the trapping potential (rather than to the spatially uniform nonlinearity coefficient)[87] and the macroscopic quantum interference and resonances have been studied in Ref. 88. Resonances in 2D and 3D BEC with periodically varying atomic scattering length has been considered in Refs. 88–90. The main issue considered in this section is a possibility of self-localization of the condensate under the action of the *ac* field.

8.1. *Averaging of the variational equations*

Let us take the mean-field GP equation for the single-particle wave function, as given by Eq. 1, without the trap:

$$i\hbar\frac{\partial\psi}{\partial t} = -\frac{\hbar^2}{2m}\nabla^2\psi + g|\psi|^2\psi\,. \tag{171}$$

We will assume the scattering length to be time-modulated so that the nonlinear coefficient in Eq. (1) takes the form

$$g = g_0 + g_1\,\sin(\chi t)\,, \tag{172}$$

where a_0 and a_1 are the amplitudes of *dc* and *ac* parts, and χ is the *ac*-modulation frequency.

Usually an external trapping potential is included to stabilize the condensate. We have omitted it because it does not play an essential role. This is also the case in some other situations, e.g. the formation of a stable Skyrmion in a two-component condensate.[91]. In fact, we will demonstrate that the temporal modulation of the nonlinear coefficient, combining the *dc* and *ac* parts as in Eq. (173) may, in a certain sense, replace the trapping potential. Another caveat concerning the present model is that, if the frequency of the *ac* drive resonates with a transition between the ground state of the condensate and an excited quasi-particle state, the mean-field description based on the GP equation will not be adequate.

We now cast Eq. (171) in a normalized form by introducing a typical frequency $\Omega \sim 2gn_0/\hbar$, where n_0 is the condensate density and rescale the time and space variables as $t' = \Omega t$ $r' = r\sqrt{2m\Omega/\hbar}$. This leads to the following equation where the $'$ have been omitted

$$i\frac{\partial\psi}{\partial t} = -\left(\frac{\partial^2}{\partial r^2} + \frac{D-1}{r}\frac{\partial}{\partial r}\right)\psi - \left[\lambda_0 + \lambda_1\sin(\omega t)\right]|\psi|^2\psi\,, \tag{173}$$

in which it is implied that ψ depends only on t and r, $D = 2$ or 3 is the spatial dimension, $\lambda_{0,1} \equiv -g_{0,1}/(\Omega\hbar)$, $\omega \equiv \chi/\Omega$.

Note that $\lambda_0 > 0$ and $\lambda_0 < 0$ in Eq. (173) correspond to the self-focusing and self-defocusing nonlinearity, respectively. Rescaling the field ψ, we will set $|\lambda_0| \equiv 1$, so that λ_0 remains a sign-defining parameter.

The next step is to apply the variational approach (VA) to Eq. (173). This approximation was originally proposed[92] and developed in nonlinear optics, first for 1D problems and, later for multi-dimensional models (see a recent review[93]). A similar technique was elaborated for the description of the multidimensional BEC dynamics based on the GP equation.[94]

To apply VA in the present case, we notice that the Lagrangian density generating Eq. (173) is

$$\mathcal{L}(\psi) = \frac{i}{2}\left(\frac{\partial\psi}{\partial t}\psi^* - \frac{\partial\psi^*}{\partial t}\psi\right) - \left|\frac{\partial\psi}{\partial r}\right|^2 + \frac{1}{2}\lambda(t)|\psi|^4\,, \tag{174}$$

where $\lambda(t) \equiv \lambda_0 + \lambda_1 \sin(\omega t)$, and the asterisk stands for the complex conjugation. The variational *ansatz* for the wave function of the condensate is chosen as the Gaussian,[92]

$$\psi_g(r,t) = A(t) \exp\left(-\frac{r^2}{2a^2(t)} + \frac{1}{2} ib(t) r^2 + i\delta(t)\right), \tag{175}$$

where A, a, b and δ are the amplitude, width, chirp and overall phase, respectively, which are assumed to be real functions of time. We did not include the degree of freedom related to the coordinate of the condensate's center as the trapping potential although not explicitly included into the model, it is assumed to prevent the motion of the condensate as a whole.

Following the standard procedure,[93] we insert the ansatz into the density (174) and calculate the effective Lagrangian,

$$L_{\text{eff}} = C_D \int_0^\infty \mathcal{L}(\psi_g) r^{D-1} dr\,, \tag{176}$$

where $C_D = 2\pi$ or 4π in the 2D or 3D cases, respectively. Finally the evolution equations for the time-dependent parameters of the ansatz (175) are derived from L_{eff} using the corresponding Euler–Lagrange equations. Subsequent analysis, as well as the results of direct numerical simulations, are presented separately for the 2D and 3D cases in the two following sections.

8.2. *Averaging of the variational equations in 2D case*

In the 2D case, the calculation of the effective Lagrangian (176) yields

$$L_{\text{eff}}^{(2\text{D})} = \pi\left(-\frac{1}{2} a^4 A^2 \dot{b} - a^2 A^2 \dot{\delta} - A^2 - a^4 A^2 b^2 + \frac{1}{4} \lambda(t)\, a^2 A^4\right), \tag{177}$$

where the overdot stands for the time derivative. The Euler–Lagrange equations following from this Lagrangian yield, the conservation of the number of atoms N in the condensate,

$$\pi A^2 a^2 \equiv N = \text{const}\,, \tag{178}$$

with the expressions for the chirp and width given by

$$\dot{a} = 2ab, \qquad \dot{b} = \frac{2}{a^4} - 2b^2 - \frac{\lambda(t) N}{2\pi a^4}\,, \tag{179}$$

and a closed-form evolution equation for the width:

$$\frac{d^2 a}{dt^2} = \frac{-\Lambda + \sigma \sin(\omega t)}{a^3}\,, \tag{180}$$

$$\Lambda \equiv 2(\lambda_0 N/(2\pi) - 2)\,, \qquad \sigma \equiv -\lambda_1 N/\pi\,. \tag{181}$$

In the absence of an *ac* component, $\sigma = 0$, Eq. (180) conserves the energy $E_{2\text{D}} = (\dot{a}^2 - \Lambda a^{-2})/2$. Obviously, $E_{2\text{D}} \to -\infty$ as $a \to 0$, if $\Lambda > 0$, and $E_{2\text{D}} \to +\infty$ as $a \to 0$, if $\Lambda < 0$. This means that, in the absence of the *ac* component, the 2D

pulse is expected to collapse if $\Lambda > 0$, and to spread out if $\Lambda < 0$. The case $\Lambda = 0$ corresponds to the critical number of particles in the condensate (the so-called "Townes soliton"). Note that a numerically exact value of the critical number is (in the present notation) $N = 1.862$ (Ref. 80), while the variational equation (181) yields $N = 2$ (if $\lambda_0 = +1$).

It is natural to consider in particular the case when the *ac* component of the nonlinear coefficient oscillates at a high frequency. In this case, Eq. (180) can be treated analytically by means of the Kapitsa averaging method. To this end, we set $a(t) = \bar{a} + \delta a$, with $|\delta a| \ll |\bar{a}|$, where $\bar{a}$ varies on a slow time scale and δa is a rapidly varying function with a zero mean value. After straightforward manipulations, we derive the following equations for the slow and rapid variables,

$$\frac{d^2}{dt^2}\bar{a} = -\Lambda(\bar{a}^{-3} + 6\bar{a}^{-5}\langle \delta a^2 \rangle) - 3\sigma\langle \delta a \, \sin(\omega t)\rangle \bar{a}^{-4}\,, \tag{182}$$

$$\frac{d^2}{dt^2}\delta a = 3\delta a \Lambda \bar{a}^{-4} + \sigma \, \sin(\omega t)\bar{a}^{-3}\,. \tag{183}$$

where $\langle \cdots \rangle$ stands for averaging over the period $2\pi/\omega$. A solution to Eq. (183) is

$$\delta a(t) = -\frac{\sigma \, \sin(\omega t)}{\bar{a}^3(\omega^2 + 3\bar{a}^{-4}\Lambda)}\,, \tag{184}$$

the substitution of which into Eq. (182) yields the final evolution equation for the slow variable,

$$\frac{d^2}{dt^2}\bar{a} = \bar{a}^{-3}\left[-\Lambda - \frac{3\Lambda\sigma^2}{(\omega^2\bar{a}^4 + 3\Lambda)^2} + \frac{3}{2}\frac{\sigma^2}{\omega^2\bar{a}^4 + 3\Lambda}\right]. \tag{185}$$

To examine whether collapse is enforced or inhibited by the *ac* component of the nonlinearity, one may consider Eq. (185) in the limit $\bar{a} \to 0$. In this limit, the equation reduces to

$$\frac{d^2}{dt^2}\bar{a} = \left(-\Lambda + \frac{\sigma^2}{6\Lambda}\right)\bar{a}^{-3}\,. \tag{186}$$

It immediately follows from Eq. (186) that, if the amplitude of the high-frequency *ac* component is large enough, $\sigma^2 > 6\Lambda^2$, the behavior of the condensate (in the limit of small $\bar{a}$) is exactly opposite to that which would be expected in the presence of the *dc* component only: in the case $\Lambda > 0$, bounce should occur rather than collapse, and vice versa in the case $\Lambda < 0$.

On the other hand, in the limit of large $\bar{a}$, Eq. (185) takes the asymptotic form $d^2\bar{a}/dt^2 = -\Lambda\bar{a}^{-3}$, which shows that the condensate remains self-confined in the case $\Lambda > 0$ i.e., if the number of atoms exceeds the critical value. This consideration is relevant if $\bar{a}$, though being large, remains smaller than the limit imposed by an external trapping potential. Thus, these asymptotic results guarantee that Eq. (185) gives rise to a stable behavior of the condensate, both the collapse and decay (spreading out) being ruled out if

$$\sigma > \sqrt{6}\Lambda > 0\,. \tag{187}$$

In the experiments with ^{7}Li with the critical number ~ 1500 atoms, for example, if we have initially 1800 atoms (i.e. $N/2\pi = 2.2$) to stabilize the condensate this means that the atomic scattering length for $\lambda_0 = 1$ should be harmonically modulated with the amplitude $\sigma = 0.98$. In fact, the conditions (187) ensure that the right-hand side of Eq. (185) is positive for small $\bar{a}$ and negative for large $\bar{a}$. This implies that Eq. (185) must give rise to a stable fixed point (FP). Indeed, when the conditions (187) hold, the right-hand side of Eq. (185) vanishes at exactly one FP,

$$\omega^2 \bar{a}^4 = \frac{3\sigma^2}{4\Lambda} + \sqrt{3\left(\frac{3\sigma^4}{16\Lambda^2} - 1\right)} - 3\Lambda\,, \tag{188}$$

which can be easily checked to be stable through the calculation of an eigenfrequency of small oscillations around it.

Direct numerical simulations of Eq. (180) produce results (not shown here) which are in exact correspondence with those provided by the averaging method, i.e., a stable state with $a(t)$ performing small oscillations around the point (188).

For the sake of comparison with the results obtained by means of an alternative approach in the next subsection, we also need an approximate form of Eq. (185) valid in the limit of small Λ (i.e., when the number of atoms in the condensate is close to the critical value) and very large ω:

$$\frac{d^2}{dt^2}\bar{a} = -\frac{\Lambda}{\bar{a}^3} + \frac{3}{2}\frac{\sigma^2}{\omega^2 \bar{a}^7}\,. \tag{189}$$

It should be noted that the Kapitsa averaging method assumes the strong nonlinearity management. Indeed $\delta a \sim (\lambda_1/\omega^2)/\bar{a}^3$. We consider $\lambda_1 \sim \omega \gg 1$, this corresponds to the strong management case. Since the averaged width $\bar{a} \sim (\lambda_1^2/(\omega^2(N - N_c))^{1/4} \sim O(1)$, we have for δa the estimate $\delta a \sim 1/\omega = \varepsilon \ll 1$ and so the correction to the averaged width is small. To calculate the value of the amplitude of the high-frequency *ac* component necessary to stop the collapse, we note that a characteristic trap frequency is $\Omega \sim 100$ Hz. So, for a modulation frequency ~ 3 kHz, which may be regarded as a typical "high modulation frequency", the dimensionless ω is ~ 30. If the initial dimensionless number of atoms is, for example, $N/2\pi = 2.2$ so that according to Eq. (181), $\Lambda = 0.4$ (this corresponds to the ^{7}Li condensate with ≈ 1800 atoms, the critical number being ≈ 1500), and the parameters of modulation are $\lambda_0 = 1$, $\lambda_1 = 2.3$, $\sigma = 10$, then the stationary value of the condensate width found from Eq. (188) is $a_{st} = 0.8l$,where $l = \sqrt{m\Omega/\hbar}$ is the healing length.

Thus the analytical approach based on the VA and the subsequent use of the assumption that the number of atoms slightly exceeds the critical value, leads to an important prediction: in the 2D case, the *ac* component of the nonlinearity, acting jointly with the *dc* one corresponding to attraction, may give rise not to collapse, but rather to a stable soliton-like oscillatory condensate state which confines itself without the trapping potential. It is relevant to mention that a qualitatively similar result, viz. the existence of stable periodically oscillating spatial cylindrical solitons

in a bulk nonlinear-optical medium consisting of alternating layers with opposite signs of the Kerr coefficient, was reported in Ref. 85, where this result was obtained in a completely analytical form on the basis of the VA, and was confirmed by direct numerical simulations. The numerical simulations confirm these predictions, as observed in Ref. 95.

The same type of equation for the soliton width can also be obtained by the moments method. Using the theory of ODE's with the periodic coefficients from Ref. 96 the conditions for the blow up and the bounded oscillations have been found. For example, for the critical case the equation for the width is

$$a_{tt} = \frac{Q_1 + Q_2 g(t)}{a^3} = \frac{p(t)}{a^3}\,, \tag{190}$$

where Q_1, Q_2 are moments of NLSE and $p(t)$ is a continuous and T-periodic function.

It was found that a necessary condition for existence of bound state is

$$\langle p \rangle = \frac{1}{T}\int_0^T p < 0\,. \tag{191}$$

The function $p(t)$ can be parametrized as $p(t) = \alpha + \beta c(t)$, with $\langle c \rangle = 0$. For the existence of the bound state it is necessary that

$$\alpha + |\beta| = 0\,. \tag{192}$$

This condition is well satisfied for the strong nonlinearity management regime with $\beta \sim 1/\varepsilon \gg 1$. The parameter α is proportional to $N - N_c$, where N_c is the critical norm and equal to the norm of the Townes soliton solution. The Townes soliton solution is the separatrix solution separating the regions of the collapsing and decaying states (see the next subsection for details). If the norm is larger than the Townes norm N_c, then the wave packet collapses, or else if the norm is lower then it decays. The numerical simulation, performed in Refs. 96 and 97 for the critical NLSE (D = 2), shows that the stabilized solution indeed exists and represents the Townes soliton with modulated parameters.

When the initial data is taken in the form of the Gaussian function, the ODEs (190) does not describe correctly the region of the existence of the bound state. Numerical simulations show that the Gaussian initial pulse ejects a significant part of the wave in the form of radiation. The remaining part of the wave packet has the form of the Townes soliton with parameters varying in time. In Ref. 98 it was proven that periodically varying any sign definite nonlinearity cannot prevent the collapse.

8.3. *Averaging of the Gross–Pitaevskii equation and Hamiltonian*

Assuming that the *ac* frequency ω is large, we rewrite the GP equation in a form,

$$i\partial\psi/\partial t + \nabla^2\psi + \lambda(\omega t)|\psi|^2\psi = 0\,. \tag{193}$$

To derive an equation governing the slow variations of the field, we use the multiscale approach, writing the solution as an expansion in powers of $1/\omega$ and introducing the slow temporal variables, $T_k \equiv \omega^{-k}t$, $k = 0, 1, 2, \ldots$, while the fast time is $\zeta \equiv \omega t$. Thus, the solution is sought for as

$$\psi(r,t) = A(r,T_k) + \omega^{-1}u_1(\zeta,A) + \omega^{-2}u_2(\zeta,A) + \cdots , \tag{194}$$

with $\langle u_k \rangle = 0$, where $\langle \cdots \rangle$ stands for the average over the period of the rapid modulation, and we assume that $\lambda_0 = +1$ (i.e., the *dc* part of the nonlinear coefficient corresponds to attraction between the atoms).

The evolution equation for the slowly varying field $A(x,T_0)$, at the order ω^{-2} is:

$$i\frac{\partial A}{\partial t} + \nabla^2 A + |A|^2 A + 2M\left(\frac{\sigma}{\omega}\right)^2 [|A|^6 A - 3|A|^4\nabla^2 A + 2|A|^2\nabla^2(|A|^2 A) + A^2\nabla^2(|A|^2 A^*)] = 0 , \tag{195}$$

where σ is the amplitude of the *ac* component. Eq. (195) is valid in both 2D and 3D cases.

For a further analysis of the 2D case, we apply a modulation theory developed in Ref. 99. The solution is searched for in the form of a modulated Townes soliton. The Townes soliton is a solution to the 2D NLS equation in the form $\psi(r,t) = e^{it}R_T(r)$, where the function $R_T(r)$ satisfies the boundary value problem

$$R_T'' + r^{-1}R_T' - R_T + R_T^3 = 0 , \qquad R_T'(0) = 0 , \qquad R_T(\infty) = 0 . \tag{196}$$

For this solution, the norm N and the Hamiltonian H take the values,

$$N_T \equiv \int_0^\infty R_T^2(r) r dr = N_c \equiv 1.862 , \qquad H_T = 0 . \tag{197}$$

To develop a general analysis, we assume that the solution with the number of atoms close to the critical value may be approximated as a modulated Townes soliton, i.e.

$$A(r,t) \approx [a(t)]^{-1} R_T(r/a(t)) e^{iS} , \qquad S = \sigma(t) + \frac{\dot{a}r^2}{4a} , \tag{198}$$

$\dot{\sigma} = a^{-2}$, with some function $a(t)$ (where the overdot stands for d/dt). If the initial power is close to the critical value, i.e., when $|N - N_c| \ll N_c$ and the perturbation is conservative, i.e.

$$\mathrm{Im} \int dV [A^* F(A)] = 0 , \tag{199}$$

as in our case, it is possible to derive an evolution equation for the function $a(t)$, starting from the approximation (198). The equation of modulation theory for width is

$$a^3 a_{tt} = -\beta_0 + \frac{\sigma^2}{4M_0\omega^2} f_1(t) , \tag{200}$$

where

$$\beta_0 = \beta(0) - \frac{\sigma^2 f_1(0)}{4M_0\omega^2}\,, \qquad \beta(0) = \frac{(N - N_c)}{M_0}\,, \tag{201}$$

and $M_0 \equiv (1/4)\int_0^\infty r^3 dr\, R_T^2 \approx 0.55$. The auxiliary function is given by

$$f_1(t) = 2a(t)\,\mathrm{Re}\left[\frac{1}{2\pi}\int dxdyF(A_T)e^{-iS}(R_T + \rho\nabla R_T(\rho))\right]. \tag{202}$$

In the lowest-order approximation, the equation takes the form

$$\frac{d^2a}{dt^2} = -\frac{\Lambda_1}{a^3} + \frac{C\sigma^2}{\omega^2 a^7}\,, \tag{203}$$

where $\Lambda_1 = (N - N_c)/M_0 - C\sigma^2/(\omega^2 a_0^4)$ and C is

$$C \equiv \frac{3}{M_0}\int_0^\infty d\rho\left[2\rho R_T^4 (R_T')^2 - \rho^2 R_T^3 (R_T')^3 - \frac{1}{8}\rho R_T^8\right] \approx 39\,. \tag{204}$$

Thus the averaged equation predicts the *arrest* of collapse by the rapid modulations of the nonlinear term in the 2D GP equation.

It should be noted that as shown in Ref. 100, in general, the averaged equation in the case of a weak nonlinearity management (corresponding to the case when in Eq. (191) parameters $\alpha, \beta \sim O(1)$), is insufficient to describe correctly the blowup domains. But in the case of the initial wave packet close in the norm to the Townes soliton solution, we are in the region of the validity of the condition (191), namely $\alpha \sim |N - N_c|/N_c \sim \varepsilon \ll 1$ and $\beta \sim O(1)$ so the bound state exist (see also Ref. 97). The numerical simulations performed in Ref. 101 has dealt with the initial wave packet taken as the Townes soliton. Since the stabilization of the soliton with the norm $N = 1.09N_c$ has been observed for σ in the interval $(5\pi, 15\pi)$ and the frequency ω in the interval $(20, 250)$, we can mention the particular value $\sigma/\omega = 8\pi/250 \approx 0.1$. Dynamical stabilization of critical NLSE in the model of 1D quintic NLSE with nonlinear management of the cubic term has been studied in Ref. 97. The numerical simulations also showed the stabilization of the initial wave packet in the form of the Townes soliton for $N = 1.08N_c$ and $\sigma = 10$, $\omega = 50$.

The evolution of the width of the soliton is described by the equation of motion of a unit mass particle in the effective anharmonic potential.

$$U_{\text{eff}} = -\frac{\Lambda_1}{2a^2} + \frac{C\sigma^2}{6\omega^2 a^6}\,. \tag{205}$$

The effect of rapid modulations of nonlinearity appears as the additional *strong repulsion* at small widths $a \sim a^{-6}$. This repulsion leads to the existence of a stable 2D bright soliton.

The same effect was observed in 1D dispersion-management for optical solitons in fibers — the Kapitsa averaging in the related *Kepler* problem leads to a new fixed point corresponding to *the dispersion-managed optical soliton*,[102–104] and the Hamiltonian averaging method in Refs. 105 and 106. Strong dispersion management can also stabilize 2D bright soliton.[107]

Let us estimate the value of the fixed point for the numerical simulations performed in Ref. 84. In this work the stable propagation of soliton has been observed for a two-step modulation of the nonlinear coefficient in 2D NLSE. The modulation of the nonlinear coefficient was $\lambda = 1 + \sigma$ if $T > t > 0$, and $\lambda = 1 - \sigma$ for $2T > t > T$. The parameters in the numerical simulations have been taken as $T = \sigma = 0.1$, $N/(2\pi) = 11.726/(2\pi)$, with the critical number as $N_c = 11.68/(2\pi)$. The map strength M is $M = \sigma^2 T^2/24$. For these values we have $a_c = 0.49$ that agreed with the value $a_c \approx 0.56$ from the numerical experiment.

Equation (195) can be written in the Hamiltonian form using the change of variables

$$q = A + M\varepsilon^2 |A|^4 A + O(\varepsilon^4)\,, \tag{206}$$

where $\varepsilon = \sigma/\omega$. In the 1D case we obtain the equation for $q(x,t)$

$$iq_t + q_{xx} + \lambda_0 |q|^2 q + 2M\varepsilon^2 [2(|q|^2)_{xx}|q|^2 + ((|q|^2)_x)^2]q = 0\,. \tag{207}$$

This equation can be written in the form $iq_t = \delta H/\delta q^*$ with the Hamiltonian

$$H = \int_{-\infty}^{\infty} dx \left[|q_x|^2 - \frac{\lambda_0^2}{2}|q|^4 + 2M\varepsilon^2 |q|^2 ((|q|^2)_x)^2 \right]. \tag{208}$$

This expression coincides $2M\varepsilon^2 = \tilde{\sigma}^2$ with the Hamiltonian obtained for the case of a strong nonlinearity management in the paper.[108,109] The discrete version of this Hamiltonian can be obtained from the Legendre transformation of the Lagrangian of the work,[110] where a weak nonlinearity management in discrete NLS lattice has been considered. Using this averaged equation in the work[108] the matter-wave solitons were found numerically. It was shown that there is no threshold on the existence of dark solitons of large amplitudes whereas such a threshold exists for bright solitons.

The averaged 2D, 3D GP equation for the case of strong nonlinearity management in the Hamiltonian form is derived recently in Ref. 100. The Hamiltonian has the form analogous to Eq. (208) and equal to

$$H = \int d^D r \left[|\nabla q|^2 - \frac{\lambda_0}{2}|q|^4 + \tilde{\sigma}^2 |q|^2 |\nabla |q|^2|^2 \right], \tag{209}$$

where $\tilde{\sigma}^2 = \int_0^1 \lambda_{-1}^2(\tau) d\tau$, $\lambda_{-1} = \int_0^1 \lambda_1 d\tau' - \int_0^1 \int_0^\tau \lambda_1 d\tau' d\tau$.

8.4. *Nonlinearity management of 2D vectorial solitons*

Analogous idea can be applied for the stabilization of 2D multicomponent BEC. The GP equation is

$$iu_{j,t} = -\frac{1}{2}\nabla^2 u_j + g(t) \left(\sum_{k=1}^{n} |u_{k,j}| \right) u_j\,, \tag{210}$$

where u_j are the wavefunctions of each of atomic species, $j = 1, \ldots, N$, $\Delta = \partial^2/\partial x^2 + \partial^2/\partial y^2$, a_{jk} are the nonlinear coupling coefficients, $g(t)$ is the periodic

function of time. This system is the extension of the Manakov system to 2D case with variable nonlinearity.

To construct solutions of the system (210) it is useful to use the stabilized scalar ($n = 1$) Townes solitons Φ_S, namely $u_j = \Phi_{S_j} = \alpha_j \Phi_S$. with the condition

$$\alpha_{j1}\alpha_1^2 + \cdots \alpha_{jn}\alpha_n^2 = 1\,, \qquad j = 1, \ldots, n\,. \tag{211}$$

By numerical simulations, it has been showed in Ref. 111 that for $n = 2; 4$ these new vector solitons remain stabilized. This showed the possibility of obtaining of the stabilized vector solitons after slow collisions of the stabilized Townes solitons. The application of such an approach for the three-dimensional vector solitons remains open.

9. Nonlinearity Management of 3D Matter Wave Soliton

Applying the methods developed in the previous section we will derive here the averaged variational equations for 3D case.

The calculation of the effective Lagrangian (176) in the 3D case yields

$$L_{\text{eff}}^{(3\text{D})} = \frac{1}{2}\pi^{3/2}A^2a^3\left[-\frac{3}{2}\dot{b}a^2 - 2\dot{\delta} + \frac{1}{2\sqrt{2}}\lambda(t)\,A^2 - \frac{3}{a^2} - 3b^2a^2\right], \tag{212}$$

as in Eq. (177). The Euler–Lagrange equations applied to this Lagrangian yield the mass conservation,

$$\pi^{3/2}A^2a^3 \equiv N = \text{const}\,, \tag{213}$$

with the expression for the chirp given by

$$\dot{a} = 2ab\,, \qquad \dot{b} = \frac{2}{a^4} - 2b^2 - \frac{\lambda(t)N}{2\sqrt{2}\pi^{3/2}a^5}\,. \tag{214}$$

The evolution equation for the width of the condensate in the normalized form is given by

$$\frac{d^2a}{dt^2} = \frac{4}{a^3} + \frac{-\Lambda + \sigma\,\sin(\omega t)}{a^4}\,, \tag{215}$$

where the amplitudes of the *dc* and *ac* components of the nonlinearity are $\Lambda \equiv 2^{-1/2}\pi^{-3/2}\lambda_0 N$ and $\sigma \equiv -2^{-1/2}\pi^{-3/2}\lambda_1 N$. In the absence of the *ac* term, $\sigma = 0$, Eq. (215) conserves the energy

$$E_{3\text{D}} = \frac{1}{2}\dot{a}^2 + 2a^{-2} - \frac{1}{3}\Lambda a^{-3}\,. \tag{216}$$

Obviously, $E_{3\text{D}} \to -\infty$ as $a \to 0$, if $\Lambda > 0$, and $E_{3\text{D}} \to +\infty$ if $\Lambda < 0$. Hence, one will have collapse or decay (spreading out) of the pulse, respectively, in these two cases.

As ω is large enough it seems natural to apply the Kapitsa's averaging method to this case too. Doing it the same way as was described in detail in the previous section for the 2D case, we find the rapidly oscillating correction $\delta a(t)$, as in Eq. (184),

$$\delta a = -\frac{\sigma\,\sin(\omega t)\bar{a}}{\omega^2\bar{a}^5 - 12\bar{a} + 4\Lambda}\,, \tag{217}$$

and then arrive at the evolution equation for the slow variable $\bar{a}(t)$ [as in Eq. (185)]:

$$\frac{d^2\bar{a}}{dt^2} = \frac{4}{\bar{a}^3} - \frac{\Lambda}{\bar{a}^4} + \frac{2\sigma^2}{\bar{a}^4(\omega^2\bar{a}^5 + 4\Lambda - 12\bar{a})}\,. \tag{218}$$

In the limit $\omega \gg 1$ the averaged equation has the form considered in Refs. 112 and 113

$$\bar{a}_{tt} = \frac{4}{\bar{a}^3} - \frac{\Lambda}{\bar{a}^4} + \frac{2\varepsilon^2}{\omega^2\bar{a}^9}\,. \tag{219}$$

Again we have the strong repulsion potential for $\bar{a} \to 0$, namely

$$U \sim \frac{\sigma^2}{\omega^2\bar{a}^8}\,. \tag{220}$$

This potential arrest the collapse of the condensate. The threshold in σ^2/ω^2 exists for the minimum of the effective potential. These predictions have been confirmed in the numerical simulations of the full 3D GP equation with time varying scattering length.[112] It is still unclear if the observed state is stable. The numerical simulations performed in Ref. 113 shows that the state is a metastable one. Predictions of the variational approach agree with the numerical data qualitatively only. After a long time the parametric instability is developed. To stabilize the soliton the dissipation can be worked on. The dissipation can be included into the GP equation by a phenomenological way[114–116]

$$i(1 - i\gamma)\hbar\psi_t = -\frac{\hbar^2}{2m}\nabla^2\psi + V_{tr}\psi + g(t)|\psi|^2\psi + i\gamma\mu\psi\,, \tag{221}$$

where γ is a phenomenological dissipation constant, which is determined experimentally, and μ is the chemical potential. It is shown by means of the numerical simulations that the state is absolutely stable. It should be noted that in distinction from the 2D case the shape is strongly deviated from the Gaussian one. It can explain why the predictions of the VA have a qualitative character only. To describe these numerical results it is necessary to develop analytical descriptions beyond of the variational one.

10. Conclusion

In summary, we present in this review the modern status of investigations of the dynamics of bright solitons in Bose–Einstein condensates. We analyze solitons in the highly elongated trap, as well as in the pancake and 3D configurations.

The formalism, as detailed above, explains recent experiments on the generation of matter wave soliton trains as the nonlinear Fresnel diffraction. We employ analytical approaches to describe the generation of trains of bright and dark solitons from weak periodic modulations of density by adiabatic variations of atomic scattering length in time. Considering recent suggestions, we have also analyzed the control of solitons in BEC, by means of variations in time and/or space of the two-atom scatering length or the trap parameters.

There are still many problems unsolved under intensive investigations. Among them, we note the following: solitons in mixed BECs like multi-components and spinor BECs,[117] solitons in Fermi–Bose mixtures,[118] nonlinearity and dispersion management for nonlinear periodic waves,[119] multidimensional solitons,[120,121] and condensates with three-body interactions.[122] Furthermore, it is also interesting to analyze the role of different nonlocalities on the soliton stability, the existence of solitons in systems with long-range interactions between atoms, nonlinear atomic interferometers with solitons, dynamics of quantum shock waves and trains of solitons using different potentials.

Acknowledgments

We are grateful to B. B. Baizakov, J. G. Caputo, R. Galimzyanov, J. Garnier, R. G. Hulet, V. V. Konotop, R. M. Kraenkel, B. A. Malomed, M. Salerno, and V. Scheshnovich for fruitful collaborations and discussions. A. Gammal and L. Tomio thank the support of Fundação de Amparo á Pesquisa do Estado de São Paulo (FAPESP) and Conselho Nacional de Desenvolvimento Científico e Tecnológico (CNPq). F. Kh. Abdullaev thanks the support of a research grant from the University of Salerno.

References

1. A. Scott, *Nonlinear Science* (Oxford University Press, Oxford, 1999).
2. P. G. Drazin and R. S. Johnson, *Solitons: An Introduction* (Cambridge University Press, Cambridge, 1989).
3. M. Remoissenet, *Waves Called Solitons: Concepts and Experiments* (Springer-Verlag, Heidelberg, 3rd rev. edn., 1999).
4. G. Eilenberger, *Solitons: Mathematical Methods for Physicists* (Springer-Verlag, Heidelberg, rev. edn., 1983).
5. S. N. Bose, *Z. Phys.* **26**, 178 (1924).
6. A. Einstein, *Sitzber. Kgl. Preuss. Akad. Wiss.* **1924**, 261 (1924); A. Einstein, *ibid.* **1925**, 3 (1925).
7. M. H. Anderson, J. R. Ensher, M. R. Matthews, C. E. Wieman and E. A. Cornell, *Science* **269**, 198 (1995).
8. K. B. Davis, M.-O. Mewes, M. R. Andrews, N. J. van Druten, D. S. Durfee, D. M. Kurn and W. Ketterle, *Phys. Rev. Lett.* **75**, 3969 (1995).
9. C. C. Bradley, A. Sackett and R. G. Hulet, *Phys. Rev. Lett.* **75**, 1687 (1995); *ibid.* **79**, 1170 (1997)(E); *ibid.* **78**, 985 (1997).
10. L. Pitaevskii and S. Stringari, *Bose–Einstein Condensation* (Clarendon Press, Oxford, 2003).
11. A. Gammal, T. Frederico, L. Tomio and Ph. Chomaz, *J. Phys. B: At. Mol. Opt. Phys.* **33**, 4053 (2000).
12. S. Burger, K. Bongs, S. Dettmer, W. Ertmer, K. Sengstock, A. Sanpera, G. V. Shlyapnikov and M. Lewenstein, *Phys. Rev. Lett.* **83**, 5198 (1999).
13. J. Denschlag, J. E. Simsarian, D. L. Feder, C. W. Clark, L. A. Collins, J. Cubizolles, L. Deng, E. W. Hagley, K. Helmerson, W. P. Reinhardt, S. L. Rolston, B. I. Schneider and W. D.Phillips, *Science* **287**, 97 (2000).
14. B. P. Anderson, P. C. Haljan, C. A. Regal, D. L. Feder, L. A. Collins, C. W. Clark and E. A. Cornell, *Phys. Rev. Lett.* **86**, 2926 (2001).

15. L. Khaykovich, F. Schrek, F. Ferrari, T. Bourdel, J. Cubizolles, L. D. Carr, Y. Castin and C. Salomon, *Science* **296**, 1290 (2002).
16. K. E. Strecker, G. B. Partrage, A. G. Truscott and R. G. Hulet, *Nature* **417**, 150 (2002).
17. K. E. Strecker, G. B. Partridge, A. G. Truscott and R. G. Hulet, *New J. Phys.* **5**, 73.1–73.8 (2003).
18. E. Fermi, *Z. Phys.* **60**, 320 (1930).
19. E. Tiesinga, A. J. Moerdijk, B. J. Verhaar and H. T. C. Stoof, *Phys. Rev.* **A46**, R1167 (1992); F. A. van Abeelen and B. J. Verharr, *Phys. Rev. Lett.* **83**, 1550 (1999).
20. V. M. Pérez García, H. Michinel and H. Herrero, *Phys. Rev.* **A57**, 3837 (1998).
21. L. D. Carr, M. A. Leung and W. P. Reinhardt, *J. Phys.* **B33**, 3983 (2000).
22. A. Gammal, T. Frederico and L. Tomio, *Phys. Rev.* **A64**, 055602 (2001); *ibid.* **A66**, 043619 (2002).
23. A. M. Kamchatnov and V. S. Shchesnovich, *Phys. Rev.* **A70**, 023604 (2004).
24. L. Salasnich, A. Parola and L. Reatto *Phys. Rev.* **A66**, 043603 (2002).
25. L. D. Carr and J. Brand, *Phys. Rev. Lett.* **92**, 040401 (2004).
26. A. M. Kamchatnov, *Nonlinear Periodic Waves and Their Modulations — An Introductory Course* (World Scientific, Singapore, 2000).
27. A. V. Gurevich and L. P. Pitaevskii, *Zh. Eksp. Teor. Fiz.* **65**, 590 (1973); *Sov. Phys. JETP* **38**, 291 (1973).
28. S. P. Novikov, S. V. Manakov, L. P. Pitaevskii and V. E. Zakharov, *Theory of Solitons: The Inverse Scattering Method* (Consultants Bureau, New York, 1984).
29. G. B. Whitham, *Linear and Nonlinear Waves* (John Wiley, New York, 1974).
30. A. M. Kamchatnov, A. Gammal and R. A. Kraenkel, *Phys. Rev.* **A69**, 063605 (2004).
31. A. M. Kamchatnov, A. Gammal, F. Kh. Abdullaev and R. A. Kraenkel, *Phys. Lett.* **A319**, 406–412 (2003).
32. A. M. Kamchatnov, R. A. Kraenkel and B. A. Umarov, *Phys. Rev.* **E66**, 036609 (2002).
33. F. Kh. Abdullaev, A. M. Kamchatnov, V. V. Konotop and V. A. Brazhnyi, *Phys. Rev. Lett.* **90**, 230402 (2003).
34. A. J. Moerdijk, B. J. Verhaar and A. Axelsson, *Phys. Rev.* **A51**, 4852 (1995).
35. S. Inouye, M. R. Andrews, J. Stenger, H.-J. Miesner, D. M. Stamper-Kurn and W. Ketterle, *Nature* **392**, 151 (1998).
36. E. Tiesinga, B. J. Verhaar and H. T. C. Stoof, *Phys. Rev.* **A47**, 4114 (1993).
37. Ph. Courteille, R. S. Freeland, D. J. Heinzen, F. A. van Abeelen and B. J. Verhaar, *Phys. Rev. Lett.* **81**, 69 (1998).
38. L. D. Carr, J. N. Kutz and W. P. Reinhardt, *Phys. Rev.* **E63**, 066604 (2001).
39. P. V. Elyutin, A. V. Buryak, V. V. Gubernov, R. A. Sammut and I. N. Towers, *Phys. Rev.* **E64**, 016607 (2001).
40. P. Meystre, *Atom Optics* (Springer-Verlag, Berlin, 2001).
41. F. Kh. Abdullaev, B. B. Baizakov, S. A. Darmanyan, V. V. Konotop and M. Salerno, *Phys. Rev.* **A64**, 043606 (2001).
42. A. Trombettoni and A. Smerzi, *Phys. Rev. Lett.* **86**, 2353 (2001).
43. V. I. Karpman and V. V. Solov'ev, *Physica* **D3**, 142 (1981).
44. J. P. Gordon, *Opt. Lett.* **8**, 596 (1983).
45. U. Al Khawaja, H. T. C. Stoof, R. G. Hulet, K. E. Strecker and G. B. Partrigde, *Phys. Rev. Lett.* **89**, 200404 (2002).
46. V. S. Gerdjikov, B. B. Baizakov and M. Salerno, On modelling of adiabatic N-solitons interactions in external potentials, cond-mat/0409741.
47. L. Salasnich, A. Parola and L. Reatto, *Phys. Rev. Lett.* **91**, 080405 (2003).

48. L. Salasnich, A. Parola and L. Reatto, *Phys. Rev.* **A65**, 043614 (2002).
49. F. Kh. Abdullaev, A. Gammal and L. Tomio, *J. Phys.* **B37**, 635 (2004).
50. D. Anderson, *Phys. Rev.* **A27**, 3135 (1983).
51. Y. Nogami and F. M. Toyama, *Phys. Rev.* **E49**, 4497 (1994).
52. V. V. Konotop, V. M. Pérez-García, Y.-F. Tang and L. Vazquez, *Phys. Lett.* **A236**, 314 (1997).
53. D. J. Frantzeskakis, G. Theocharis, F. K. Diakonos, P. Schmelcher and Y. S. Kivshar, *Phys. Rev.* **A66**, 053608 (2002).
54. L. A. Nesterov, *Opt. Spectrosk.* **64**, 694 (1988).
55. A. B. Aceves, J. V. Moloney and A. C. Newell, *Phys. Rev.* **A39**, 1809 (1989); *ibid.* **A39**, 1828 (1989).
56. A. Gammal, L. Tomio and T. Frederico, *Phys. Rev.* **A66**, 043619 (2002).
57. A. A. Sukhorukov, Yu. S. Kivshar, O. Bang, J. J. Rasmussen and P. L. Christiansen, *Phys. Rev.* **E63**, 036601 (2001).
58. A. Gammal, T. Frederico, L. Tomio and F. Kh. Abdullaev, *Phys. Lett.* **A267**, 305 (2000).
59. T. Tsurumi and M. Wadati, *J. Phys. Soc. Jpn.* **68**, 1531 (1999).
60. Y. S. Kivshar, F. Zhang and L. Vazquez, *Phys. Rev. Lett.* **67**, 1177 (1991).
61. T. I. Lakoba and D. J. Kaup, *Phys. Rev.* **E56**, 6147 (1997).
62. R. H. Goodman, P. J. Holmes and M. I. Weinstein, *Physica* **D161**, 21 (2002).
63. F. K. Fatemi, K. M. Jones and P. D. Lett, *Phys. Rev. Lett.* **85**, 4462 (2000).
64. B. B. Baizakov, G. Filatrella, B. Malomed and M. Salerno, *Phys. Rev.* **E71**, 036619 (2005).
65. F. Kh. Abdullaev and R. M. Galimzyanov, *J. Phys.* **B36**, 1099 (2003).
66. F. Kh. Abdullaev and M. Salerno, *J. Phys.* **B36**, 2851 (2003).
67. H. E. Nistazakis, D. J. Frantzeskakis, N. Brouzakis, F. K. Diakonos, P. Schmelcher and J. Schmiedmayer, Time-dependent trapping of solitons in Bose–Einstein condensates, cond-mat/0211702.
68. W. P. Reinhardt and C. W. Clark, *J. Phys.* **B30**, L785 (1997).
69. M. L. Quiroga-Teixero, D. Anderson, P. A. Andrekson, A. Berntson and M. Lisak, *J. Opt. Soc. Am.* **13**, 687 (1996).
70. V. I. Karpman, *Phys. Scr.* **20**, 462 (1979).
71. A. I. Maĭmistov, *Zh. Eksp. Teor. Fiz.* **104**, 3620 (1993); *Sov. Phys. JETP* **77**, 727 (1993).
72. G. Theocharis, P. Schmelcher, P. K. Kevrekidis and D. Frantzeskakis, Matter-wave solitons in collisionally inhomogeneous condensates, cond-mat/0505127.
73. F. Kh. Abdullaev, A. A. Abdumalikov and B. B. Baizakov, *Kvant. Elektron.* **24**, 176 (1997).
74. F. Kh. Abdullaev and J. Garnier, *Phys. Rev.* **A70**, 053604 (2004).
75. F. Kh. Abdullaev, A. A. Abdumalikov and B. B. Baizakov, *Opt. Commun.* **138**, 49 (1997).
76. Z. Liang, Z. Zhang and W. Liu, *Phys. Rev. Lett.* **94**, 050402 (2005).
77. N. Akhmediev and A. Ankiewicz, *Solitons: Nonlinear Pulses and Beams* (Chapman–Hall, London, 1997).
78. F. Kh. Abdullaev, S. A. Darmanyan and P. K. Khabibullaev, *Optical solitons* (Springer-Verlag, Berlin, 1993).
79. V. P. Barros, M. Brtka, A. Gammal and F. Kh. Abdullaev, submitted to Journal of Physics B.
80. L. Bergé, *Phys. Rep.* **303**, 259 (1998).
81. S. L. Cornish, N. R. Claussen, J. L. Roberts, E. A. Cornell and C. E. Wieman, *Phys. Rev. Lett.* **85**, 1795 (2000).

82. Y. Kagan, E. L. Surkov and G. V. Shlyapnikov, *Phys. Rev. Lett.* **79**, 2604 (1997).
83. F. Kh. Abdullaev, J. G. Caputo, R. A. Kraenkel and B. A. Malomed, *Phys. Rev.* **A67**, 013605 (2003).
84. L. Bergé, V. K. Mezentsev, J. Juul Rasmussen, P. L. Christiansen and Yu. B. Gaididei, *Opt. Lett.* **25**, 1037 (2000).
85. I. Towers and B. A. Malomed, *J. Opt. Soc. Am.* **B19**, 537 (2002).
86. Y. Silberberg, *Opt. Lett.* **15**, 1281 (1990); B. A. Malomed, P. Drummond, H. He, A. Berntson, D. Anderson and M. Lisak, *Phys. Rev.* **E56**, 4725 (1997).
87. R. Dum, A. Sampera, K. Suominen, M. Brewczyk, M. Kus, K. Rzazevski and M. Lewenstein, *Phys. Rev. Lett.* **80**, 3899 (1998).
88. F. Kh. Abdullaev and R. A. Kraenkel, *Phys. Lett.* **A272**, 395 (2000).
89. F. Kh. Abdullaev, J. Bronski and R. Galimzyanov, *Physica* **D184**, 319 (2003).
90. S. K. Adhikari, *J. Phys.* **B35**, 2831 (2002); *ibid.* **B36**, 1109 (2003).
91. R. A. Battye, N. R. Cooper and P. M. Sutcliffe, *Phys. Rev. Lett.* **88**, 080401 (2002).
92. D. Anderson, *Phys. Rev.* **A27**, 1393 (1983).
93. B. A. Malomed, *Progress in Optics* **43**, 69 (2002).
94. V. M. Pérez-García, H. Michinel, J. I. Cirac, M. Lewenstein and P. Zoller, *Phys. Rev.* **A56**, 1424 (1997).
95. H. Saito and M. Ueda, *Phys. Rev. Lett.* **90**, 040403 (2003).
96. G. D. Montesinos, V. M. Perez-Garcia and P. Torres, *Physica* **D191**, 193 (2004).
97. F. Kh. Abdullaev and J. Garnier, arXive:cond-mat/0507042.
98. V. V. Konotop and P. Pacciani, *Phys. Rev. Lett.* **94**, 240405 (2005).
99. G. Fibich and G. C. Papanicolaou, *Phys. Lett.* **A239**, 167 (1998); *SIAM J. Appl. Math.* **60**, 183 (1999).
100. P. G. Kevrekidis, A. Stefanov and D. E. Pelinovsky, arXive:cond-mat/0505498.
101. G. D. Montesinos and V. M. Perez-Garcia, *Math. Comp. Simul.* **69**, 447 (2005).
102. J. H. B. Nijhof, N. J. Doran, W. Forysiak and F. M. Knox, *Electron. Lett.* **33**, 1726 (1997).
103. I. Gabitov and S. K. Turitsyn, *Opt. Lett.* **21**, 327 (1996).
104. F. Kh. Abdullaev and J. G. Caputo, *Phys. Rev.* **E58**, 6637 (1998).
105. S. K. Turitsyn, A. B. Aceves, C. K. R. T. ones, *Phys. Rev.* **E58**, R48 (1998).
106. J. Garnier, *Opt. Commun.* **206**, 411 (2002).
107. F. Kh. Abdullaev, B. B. Baizakov and M. Salerno, *Phys. Rev.* **E68**, 066605 (2003).
108. D. E. Pelinovsky, P. G. Kevrekidis, D. J. Frantzeskakis and V. Zharnitsky, *Phys. Rev.* **E70**, 047604 (2004).
109. V. Zharnitsky and D. Pelinovsky, *Chaos*, in press (2005).
110. F. Kh. Abdullaev, E. N. Tsoy, B. A. Malomed and R. A. Kraenkel, *Phys. Rev.* **A68**, 053606 (2003).
111. G. D. Montesinos, V. M. Pérez-García and H. Michinel *Phys. Rev. Lett.* **92**, 133901 (2004).
112. S. K. Adhikari, *Phys. Rev.* **A69**, 063613 (2004).
113. H. Saito and M. Ueda, *Phys. Rev.* **A70**, 053610 (2004).
114. L. P. Pitaevskii, *Zh. Eksp. Teor. Fiz.* **35**, 408 (1958); *Sov. Phys. JETP* **35**, 382 (1959).
115. S. Choi, S. A. Morgan and K. Burnett, *Phys. Rev.* **A57**, 4057 (1998).
116. M. Tsubota, K. Kasamatsu and M. Ueda, *Phys. Rev.* **A65**, 023603 (2002).
117. J. Ieda, T. Miyakawa and M. Wadati, *Phys. Rev. Lett.* **93**, 194102 (2004).
118. T. Karpiuk, M. Brewczyk, S. Ospelklaus-Schwarzer, K. Bongs, M. Gajda and K. Rzazewski, *Phys. Rev. Lett.* **93**, 100401 (2004).

119. V. V. Kartashov, V. A. Visloukh, E. Marti-Panameno, D. Artigas and L. Torner, *Phys. Rev.* **E68**, 046609 (2003).
120. S. K. Adhikari, *Phys. Rev.* **E71**, 016611 (2005).
121. M. Trippenbach, M. Matuszewski and B. A. Malomed, *Europhys. Lett.* **70**, 8 (2005).
122. F. Kh. Abdullaev, Dynamical stabilization of matter-wave solitons in BEC with three body interactions, NLGW, OSA, Technical dijest, Dresden, (2005).